Syst. Biol. 54(6):916–935, 2005

ISSN: 1063-5157 print / 1076-836X online
DOI: 10.1080/10635150500354837

Molecular Phylogenetics of the Siphonophora (Cnidaria), with Implications for the Evolution of Functional Specialization

CASEY W. DUNN,[1,4] PHILIP R. PUGH,[2] AND STEVEN H. D. HADDOCK[3]

[1]*Department of Ecology and Evolutionary Biology, Yale University, New Haven, Connecticut, USA*
[2]*National Oceanography Centre, Southampton, SO14 3ZH, UK; E-mail: prp@noc.soton.ac.uk*
[3]*Monterey Bay Aquarium Research Institute, 7700 Sandholdt Road, Moss Landing, California 95039-0628, USA; E-mail: haddock@mbari.org*
[4]*Current Address: Kewalo Marine Laboratory, 41 Ahui St., Honolulu, Hawaii 96816, USA; E-mail: cdunn@hawaii.edu*

Abstract.— Siphonophores are a group of pelagic colonial hydrozoans (Cnidaria) that have long been of general interest because of the division of labor between the polyps and medusae that make up these "superorganisms." These polyps and medusae are each homologous to free living animals but are generated by an incomplete asexual budding process that leaves them physiologically integrated. They are functionally specialized for different tasks and are precisely organized within each colony. The number of functional types of polyps and medusae varies across taxa, and different authors have used this character to construct phylogenies polarized in opposite directions, depending on whether they thought siphonophore evolution proceeded by a reduction or an increase in functional specialization. We have collected taxa across all major groups of siphonophores, many of which are found exclusively in the deep sea, using remotely operated underwater vehicles (ROVs) and by SCUBA diving from ships in the open ocean. We have used 52 siphonophores and four outgroup taxa to estimate the siphonophore phylogeny with molecular data from the nuclear small subunit ribosomal RNA gene (18S) and the mitochondrial large subunit ribosomal RNA gene (16S). Parsimony reconstructions indicate that functionally specialized polyps and medusae have been gained and lost across the phylogeny. Maximum likelihood and Bayesian analyses of morphological data suggest that the transition rate for decreased functional specialization is greater than the transition rate for increased functional specialization for three out of the four investigated categories of polyps and medusae. The present analysis also bears on several long-standing questions about siphonophore systematics. It indicates that the cystonects are sister to all other siphonophores, a group that we call the Codonophora. We also find that the Calycophorae are nested within the Physonectae, and that the Brachystelia, a historically recognized grouping of short-stemmed taxa, are polyphyletic. [Cnidaria; colonial animals; deep sea; division of labor; functional specialization; Hydrozoa; phylogenetics; Siphonophores.]

The siphonophores (Figs. 1 and 2), a group of about 170 described species of pelagic hydrozoans (Cnidaria), are arguably the most complex of all colonial animals (Beklemishev, 1969). Each colony arises by a highly regulated budding process that arranges polyps and medusae in a precise, species-specific pattern (Dunn, 2005). These polyps and medusae, which are also called zooids, are physiologically integrated and fall into discrete functional categories. The zooids of these different categories are each specialized for tasks such as locomotion, feeding, defense, excretion, or reproduction. The colonial organization and degree of functional specialization varies across siphonophore species. This division of labor was of central interest to many of the most influential zoologists of the 19th century, inspiring Gegenbaur (1859), Huxley (1859), Haeckel (1888), and others to write lengthy monographs on siphonophore morphology, systematics, and phylogeny. They were largely motivated by the belief that the division of labor within siphonophores has important general implications, as Haeckel (1869) discussed at length when he drew parallels between the functional specialization of zooids in siphonophore colonies, cells in multicellular organisms, and even workers in an industrialized society. The unique colonial individuality that siphonophores possess led Mackie (1963) to call them "superorganisms."

There has been much speculation regarding the evolution of siphonophores, with some authors arguing that there has been a trend towards an increased number of zooid types (e.g., Haeckel, 1869) and others believing that the common ancestor of siphonophores had the greatest number of zooid types and that the existing diversity is a result of differential zooid loss (e.g., Stepanjants, 1967). It has not been possible in the past to test these hypotheses because there has been considerable confusion regarding the phylogeny of siphonophores, with investigators advocating very different topologies and polarities (reviewed by Mackie et al., 1987). Siphonophores have traditionally been divided into three groups (Fig. 2), the Cystonectae (with a pneumatophore and siphosome), Physonectae (with a pneumatophore, nectosome, and siphosome), and Calycophorae (with a nectosome and siphosome). A previous investigation of the hydrozoan phylogeny based on the nuclear small subunit ribosomal RNA (18S) included nine siphonophore species (Collins, 2000, 2002). It indicated that siphonophores are monophyletic and nested within the Hydrozoa, and that *Physalia*, a cystonect, is sister to the other sampled siphonophores. The included taxa were not sufficient to determine whether the cystonects are paraphyletic and give rise to the other siphonophores, or are monophyletic and sister to the other siphonophores. This previous study also suggested that the physonects are paraphyletic and give rise to the Calycophorae, though support for the relevant node was not strong. There were too few taxa to investigate the evolution of functional specialization in siphonophores.

The primary limitation to working with siphonophores, and the reason that so little is known about them, is that they are extremely difficult to collect. All siphonophores are oceanic, and none are

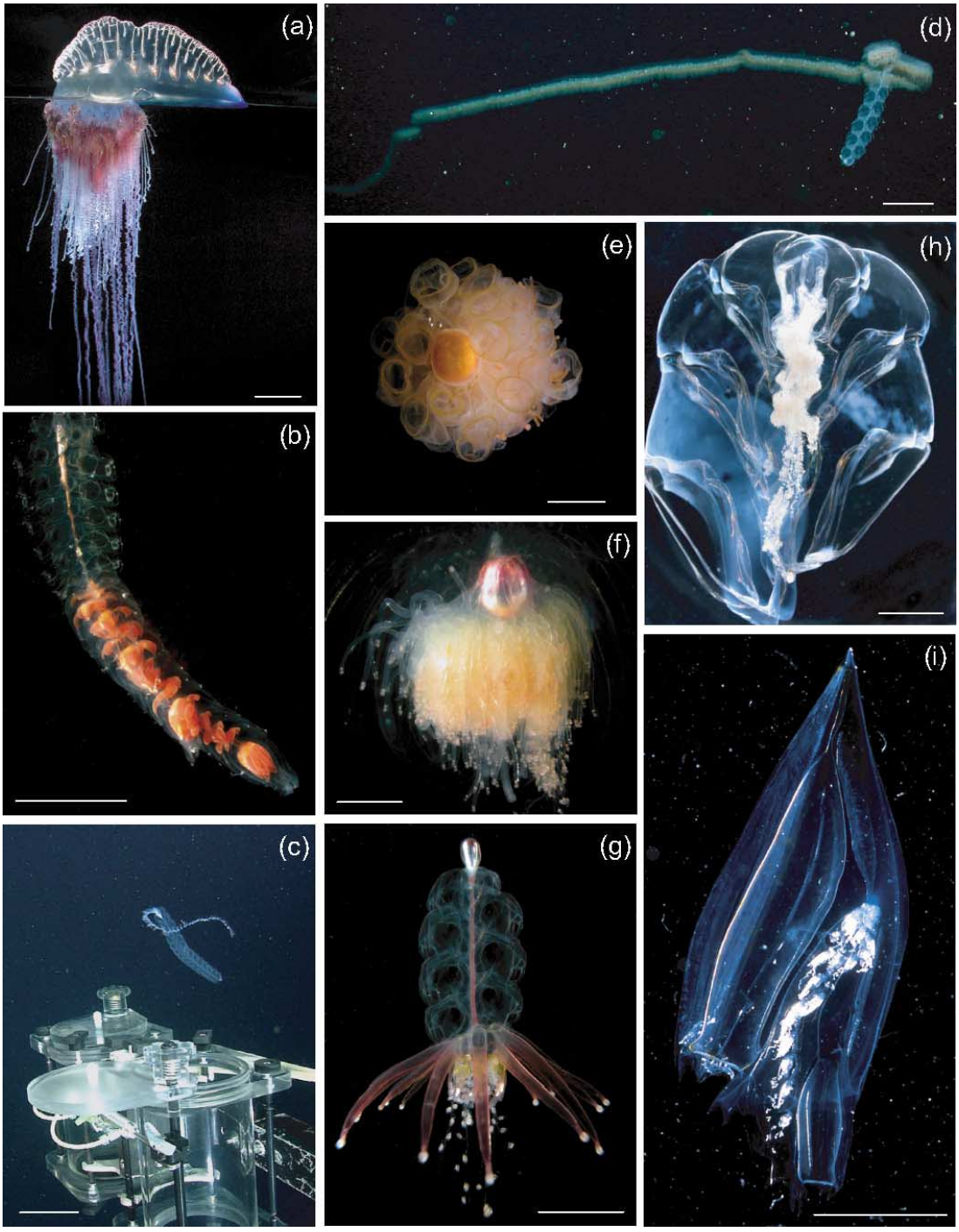

FIGURE 1. Photographs of representatives of the major groups of siphonophores taken in situ and aboard research ships. Views are lateral with the anterior end pointing up unless otherwise noted. Scale bars are approximate. (a) *Physalia physalis*, scale bar = 5 cm. Also known as the Portuguese Man o' War, this familiar siphonophore is unique in that it lives at the air-water interface and has a hypertrophied pneumatophore that acts as a sail. (b) *Stephanomia amphytridis*, scale bar = 5 cm. Pigment in the gastrovascular fluid colors the stem and polyps of the siphosome orange. The transparent structures sheathing the siphosome are bracts. (c) *Bargmannia elongata*, scale bar = 10 cm. The anterior end points to the lower right. This photograph was taken just before collection by the remotely operated underwater vehicle *Ventana* (Monterey Bay Aquarium Research Institute). The cylindrical samplers are visible in the lower part of the pane. (d) *Apolemia* sp., scale bar = 10 cm. The anterior end, which is in the right of the frame, is pointed downward. Some *Apolemia* reach more than 30 m in length. (e) *Stephalia dilata*, scale bar = 1 cm, view from above (anterior end facing out of the page). The large pneumatophore, which is orange, can be seen surrounded by the nectophores. This is a short-stemmed species. (f) *Athorybia rosacea*, scale bar = 0.5 cm. A paedomorphic, short-stemmed species. The *Athorybia* are the only codonophore taxa to lack nectophores, which they have secondarily lost. (g) *Physophora hydrostatica*, scale bar = 2 cm. A short-stemmed species with a conspicuous whorl of palpons above the gastrozooids. This species lacks bracts at maturity. (h) *Hippopodius hippopus*, scale bar = 1 cm. A prayomorph calycophoran. The stem, which is white, is retracted between the six identical nectophores, the youngest of which are at the anterior end. (i) *Diphyes dispar*, scale bar = 1 cm. This diphyomorph calycophoran has a well-differentiated anterior and posterior nectophore. The stem is retracted within the anterior nectophore. Pane (a) is a cystonect siphonophore. All other specimens belong to the Codonophora, a clade we describe here that is composed of the grade Physonectae (b to g) and the clade Calycophorae (h to i).

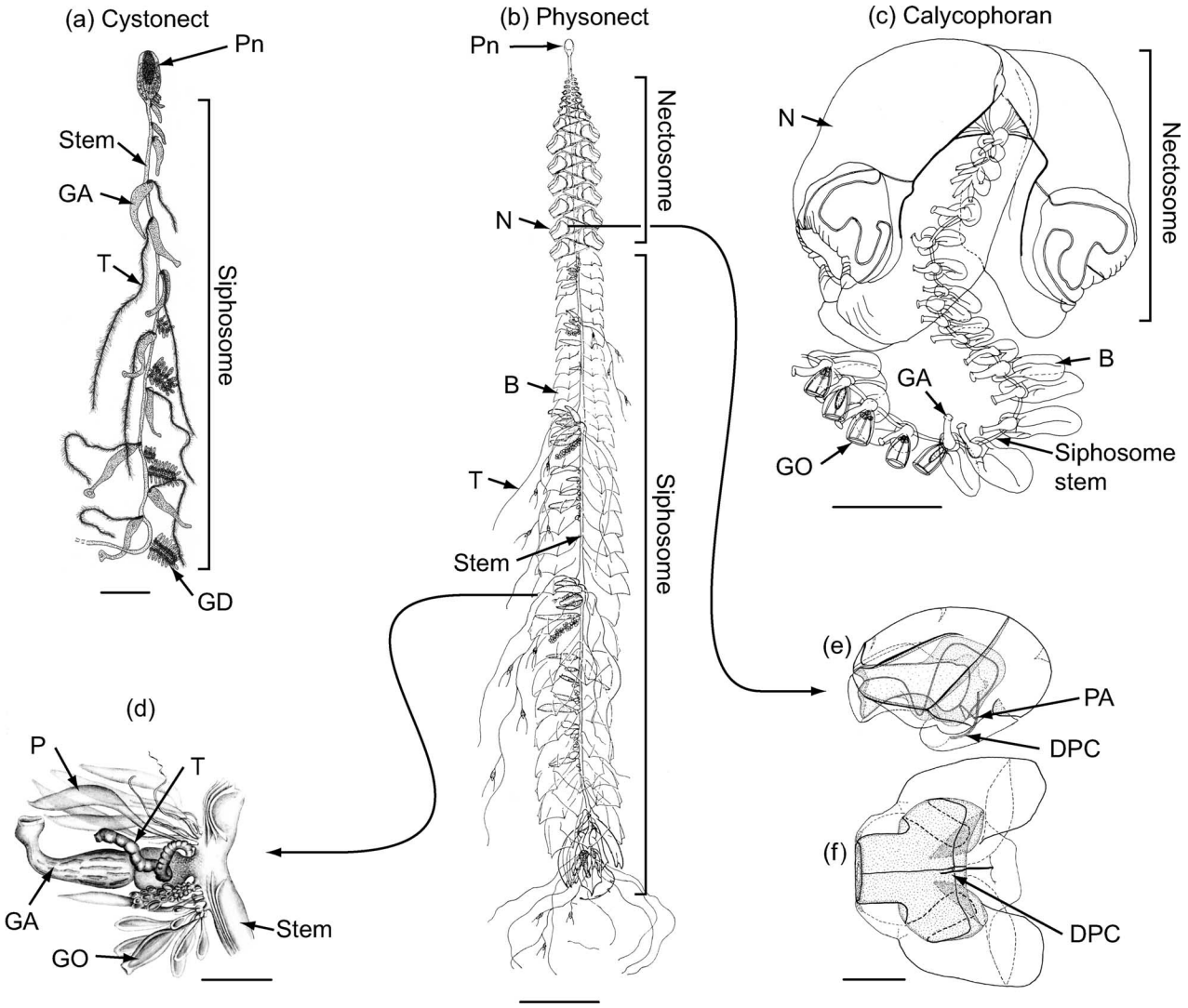

FIGURE 2. Diagrams of siphonophore structure. The anterior end is up unless otherwise noted. The stem can be divided into two regions, the nectosome (which bears the nectophores that propel the entire colony) and the siphosome (which bears all other zooids). Scale bars are approximate. (a) A cystonect, *Rhizophysa eysenhardti*, scale bar = 2 cm (adapted from Kawamura, 1910). Cystonects have a pneumatophore and a siphosome, but no nectosome. (b) *Agalma elegans*, scale bar = 2 cm (adapted from Totton, 1954). This species has traditionally been placed in the Physonectae, a grade taxon that includes species with a nectosome (except *Athorybia*), a siphosome, and a pneumatophore. (c) A calycophoran, *Rosacea flaccida*, scale bar = 1 cm (adapted from Biggs et al., 1978). Calycophorans have a nectosome and a siphosome, but no pneumatophore. (d) Lateral view of a portion of siphosomal stem from the physonect *Agalma okeni* (adapted from Bigelow, 1911) showing some zooids in detail, scale bar = 2 mm. The figured region is part of a series that repeats, with only slight differences, along the entire length of the siphosome. Lateral view (e) and view from the lower surface (f) of a detached nectophore of *Halistemma rubrum*, scale bar = 5 mm. Nectophores are medusae that are specialized for propulsion, and contraction causes water to exit from ostium, which faces to the left in these figures. The nectosac (subumbrella) is indicated by stippling. Nourishment is provided from the stem by a series of canals, which sometimes include the descending pallial canal (DPC). The point of attachment (PA) to the stem is also shown. B, bract; GA, gastrozooid; GD, gonodendron (a compound reproductive structure consisting of gonophores, palpons, and special nectophores that propel detached gonodendra but not the entire colony); GO, gonophore; N, nectophore; P, palpon; Pn, pneumatophore; T, tentacle (of the gastrozooid).

permanently attached to a substrate; instead, most are free swimming in the water column. They are among the most abundant members of the macroplankton and are widely distributed in the open ocean (Gasca, 2002; Pagès and Gili, 1992). Siphonophores include the longest animals in the world; some specimens can exceed 40 m in length (Robison, 1995). They are, however, very fragile and many are found only in the deep sea (Dunn et al., 2005; Haddock et al., 2005). Nets have been used to trawl for the deeper species, but most are reduced to unidentifiable gelatinous pieces or pass straight through the mesh. Other species have sometimes been dipped from the surface of the water on transoceanic voyages or at several exceptional locations where they can sometimes be found close to the coast, such as Villefranche-Sur-Mer, France.

In order to resolve long-standing questions about siphonophore systematics, and to trace the evolution

of functional specialization between zooids, we have estimated the siphonophore phylogeny using 52 taxa sampled across all major siphonophore groups with molecular sequence data from 18S and the mitochondrial large subunit ribosomal RNA gene (16S). This was possible because we were able to take advantage of modern oceanic collection techniques. We collected species that occur near the surface using blue-water SCUBA diving, a protocol that allows divers working from research ships to collect in the upper part of the water column far from shore (Hamner, 1975). We collected deeper species with sampling canisters (Youngbluth, 1984) mounted on remotely operated underwater vehicles (ROVs) and used two specimens similarly collected by a manned submersible.

Materials and Methods

Specimens Examined

Specimens were collected by blue-water diving, remotely operated underwater vehicles, and manned submersibles from oceanic research vessels and at the Station Zoologique in Villefranche-Sur-Mer, France. Physical vouchers were taken of specimens whenever possible. These are housed at the Monterey Bay Aquarium Research Institute in Moss Landing, California; El Colegio de la Frontera Sur (ECOSUR) in Chetumal, Mexico; and the Yale Peabody Museum (YPM) in New Haven, Connecticut. Photographs were taken of most specimens that were too small, fragile, or damaged for physical preservation, and these were also deposited at the YPM. Tissues for molecular analysis were stored frozen at −80°C. The 18S sequence for *Physalia physalis* is from Collins (2000, GenBank accession number AF358065).

Six specimens included here are of distinct species that have not yet been described. These have been given temporary names that indicate their affinity, as closely as possible, to known taxa. The name *Stephanomia amphytridis*, as used here, is synonymous with the species Totton (1936) referred to as *S. amphitridis* [sic] and later as *?Halistemma amphytridis* (Totton, 1965). The specimens referred to by Totton are still extant and have been reexamined. We are using the original name because this taxon does not seem to be allied with the other species now placed in *Halistemma*. This species is not the same as that recently redescribed by Mapstone (2004) under the name *H. amphytridis*.

Four non-siphonophore outgroup taxa were included in the present analysis. These taxa were chosen because they were previously shown to be more closely related to the siphonophores than other sampled hydrozoans (Collins, 2000). We collected *Velella velella* and *Porpita porpita* and sequenced 16S from this new material. Previously published sequence data were used for *V. velella* 18S (Collins, 2002, GenBank AF358087), *P. porpita* 18S (Collins, 2002, AF358086), *Staurocladia wellingtoni* 18S (Collins, 2002, AF358084), *S. wellingtoni* 16S (Schuchert, 2005, AJ580934), *Hydra circumcincta* 18S (Medina et al., 2001, AF358080), and *H. vulgaris* 16S (Pont-Kingdon et al., 2000, AF100773).

Molecular Methods

Total DNA was prepared with the DNeasy Tissue Kit (Qiagen) according to the supplied instructions. Gene fragments were amplified with polymerase chain reaction (PCR). The primers from Medlin et al. (1988) were used for 18S. They amplify almost the full length of the gene. The primers for 16S, which amplify portions of domains IV and V, are from Cunningham and Buss (1993). Each PCR reaction consisted of 5 μl 10 × PCR Buffer II (Applied Biosystems), 0.2 μl Amplitaq polymerase (Applied Biosystems), 1 μl 10 mM (each) dNTP, 5 μl 25 mM $MgCl_2$, 2.4 μl 10 μM forward primer, 2.4 μl 10 μM reverse primer, 1 μl template, and water to a total volume of 50 μl. Both genes were amplified with an initial denaturation step at 94°C for 2 min followed by 30 cycles of 30 s at 94°C, 1 min at the annealing temperature, and 1 min at 72°C. There was then a final extension for 5 min at 72°C. An annealing temperature of 40°C was used for 18S and an annealing temperature of 50°C was used for 16S.

PCR reactions were cleaned using QIAquick PCR Purification Kit (Qiagen) and sequenced on an ABI 3100 (Applied Biosystems) using BigDye v3.0 (Applied Biosystems), or sent to SeqWright (Houston, Texas) for cleaning and cycle sequencing. All PCR products were sequenced at least once in each direction. The 16S sequencing reactions were initiated with the amplification primers and 18S was sequenced with the primers specified by Collins (2000). Contiguous sequences were assembled with Sequencher 3.1.1 (Gene Codes Corporation).

Alignment

Sequences for each gene were first aligned with T-Coffee (Notredame et al., 2000). The different magnitudes of variation present in each gene necessitated different alignment strategies from this point on.

The secondary structure of human 18S, based on direct empirical evidence and available at the Comparative RNA website (http://www.rna.icmb.utexas.edu; Cannone et al., 2002), was hand-coded in DCSE format (De Rijk and De Wachter, 1993) onto the *Agalma elegans* 18S sequence. MFold v3.0 (Zuker, 2003) was used to estimate the secondary structure of regions of the *A. elegans* 18S sequence that could not be confidently aligned to the human 18S sequence. Default MFold settings were used except that the temperature was set to 20°C. The secondary structure of *A. elegans* 18S was then visualized with RNAviz 2.0 (De Rijk et al., 2003) and used to determine the structural context of problems in the siphonophore 18S alignment. These issues were then manually resolved in MacClade v4.06 (Maddison and Maddison, 2003).

Because 16S was more variable than 18S, it was a lengthier process to determine whether a hypothesized alignment for this gene was consistent with a particular secondary structure. A Perl script, *secondchance* (available online, along with the other supplementary materials, at http://systematicbiology.org), was written to

partially automate this process. It imports a sequence alignment matrix using several BioPerl modules (Stajich et al., 2002), and then opens a separate file that contains secondary structure information for one of the sequences in the alignment. It propagates this secondary structure information across all the other sequences in the matrix, according to the alignment, and exports them in DCSE format for further visualization. The improvement of the alignment was an iterative process that started by using *secondchance* to map the secondary structure information from *Hydra* (Pont-Kingdon et al., 2000) onto all the sequences in the 16S alignment. The alignment matrix was then manually modified to improve the consistency of the alignment with the structural model, and again visualized with the aid of *secondchance*.

Because the secondary structure of 16S was extrapolated from the *Hydra* structure, which is itself an extrapolation from the empirically derived structural model for *Escherichia coli* large subunit ribosomal RNA, independent evidence was sought to confirm that the siphonophore structural model was reasonably accurate. This was accomplished with the program Circles (Page, 2000), which uses mutational covariance between sites to infer base pairings and reconstruct secondary structure according to this variation.

Phylogenetic Analysis

Default settings were used for all phylogenetic programs unless otherwise noted. The congruence of the 16S and 18S data sets was tested using the ILD test (Farris et al., 1995) as implemented in PAUP* 4.0b10 (Swofford, 2003). Maximum parsimony (MP) and maximum likelihood (ML) analyses were also done with PAUP*. These searches were unrooted, and trees were visualized with TreeView (Page, 1996).

Gaps were treated as missing data and all characters were equally weighted in the MP analysis. For each data set (16S, 18S, and combined), 1000 random sequence addition MP heuristic searches were run. These searches were followed by 1000 bootstrap replicates, each with 10 random addition MP heuristic searches limited to one hour.

The likelihood ratio test, as implemented in ModelTest 3.06 (Posada and Crandall, 1998), was used to select a molecular evolution model for the 16S, 18S, and combined data sets. Fifty random addition ML heuristic searches were conducted on each data set. These were then followed by 100 bootstrap replicates, each with two random addition ML heuristic searches limited to 1 h.

MrBayes v3.0b4 (Ronquist and Huelsenbeck, 2003) was used for Bayesian phylogenetic inference, following model selection by MrModelTest (Nylander, 2002). Trees were sampled every 100 generations. All parameters except topology were unlinked between the 16S and 18S partitions in the combined analysis. To verify convergence, six searches were conducted on each data set. Five of these searches were run for 2 million generations each and one was run for 10 million generations. All parameters from each run were visually inspected with Tracer v1.0.1 (Rambaut and Drummond, 2003) to determine the number of generations until burn-in. The consensus trees of the different runs on a given data set were compared to see if they had converged on the same topology. Post–burn-in trees were combined across all runs for a given dataset, and were considered to have been drawn from the same posterior distribution for all further analyses.

Hypothesis Testing

Topological hypotheses suggested by previous systematic work, but that were not consistent with the trees recovered in the present analyses, were tested using the SOWH parametric bootstrap test (Goldman et al., 2000; Hillis et al., 1996; Huelsenbeck et al., 1996). The test was implemented by first using 25 constrained ML searches in PAUP* to infer branch lengths under the topology of the null hypothesis. The GTR+I+Γ model was used. One hundred data sets were simulated with seq-gen (Rambaut and Grassly, 1997) under this tree and model. Ten unconstrained MP searches and 10 MP searches constrained to the null hypothesis were then conducted on each simulated data set. The set of differences between the scores of the best constrained tree and the best unconstrained tree for each simulated data set was used as an estimate of the null distribution.

Morphological Observations and Character Evolution

Morphological character data follow Totton (1965), except where more recent revisions were available (Pugh, 1983, 1992, 1999, 2001, 2003) or a previous treatment was more thorough (e.g., Totton, 1960). Data not available in the literature were obtained by examining the voucher specimens for this study and other material in the collection of PRP. The most parsimonious explanation for the histories of morphological characters were inferred, and visualized, using Mesquite (Maddison and Maddison, 2004) under default settings. The numbers of zooid types were scored as ordered characters for bracts, gastrozooids, and palpons. Nectophores were scored as none, one of one type, two of one type, many (>2) of one type, or two of two types.

ML and Bayesian methods were also used to investigate gain and loss of zooids. Nectophores were scored differently than in the parsimony analyses, with only the number of types of nectophores being taken into consideration. A posterior distribution of trees was generated with MrBayes using the combined, unpartitioned molecular data set. The chain was run for 10 million generations and sampled every 20,000 generations. Five additional runs, each of 2 million generations, were also analyzed to make sure that all converged on the same region of treespace. Mesquite was used to remove the outgroup from the post burn-in posterior distribution of trees. Morphological transition rates were constrained to either two rates, one for zooid gain (α) and one for zooid loss (β), or to one rate, where all transition rates are the same ($\alpha = \beta$). This nomenclature follows that of McShea and Venit (2002). Bracts, nectophores, gastrozooids, and palpons were each analyzed separately. BayesMultiState

(Pagel et al., 2004) was used in ML mode to calculate the likelihood of the morphological data given either a one-rate or two-rate model of character evolution. This was carried out for all trees in the posterior distribution generated by MrBayes. The arithmetic mean of the log likelihoods was then used in a likelihood ratio test with one degree of freedom to see if the two-rate model was a significantly better fit to the data than the one-rate model for each zooid type.

A one-rate ($\alpha = \beta$) prior was estimated from the one-rate likelihood surface of each of the four zooid types. This is the "intermediate prior" of Pagel et al. (2004). The consensus of the posterior distribution of trees was used for these calculations (with the outgroup pruned away). The log likelihood of the morphological data was calculated with BayesMultiState for 100 different rates from zero to some maximum value that was verified to be on the right tail of the distribution. *lsurface*, a Perl wrapper for BayesMultiState (available in the online supplemental materials), was used to automate rate variation and score parsing. The log likelihoods of the distribution were transformed to likelihoods and used to calculate the weighted means and variances of the rate parameters. Once the priors were in hand, BayesMultiState was used in MCMC mode to estimate the posterior distribution of the rates for each zooid type. The rate matrix was constrained such that the posterior distributions of α and β (the rates of zooid gain and loss) were estimated separately, but under the same prior. BayesMultiState MCMC runs were sampled every 100 generations for 5 million generations after a 5000-generation burn-in.

RESULTS

Collection, Sequencing, and Alignment

Specimens were collected in the eastern North Pacific, Gulf of California, western North Atlantic, and northern Mediterranean (Fig. 3; Table 1). All sequence data have been deposited in Genbank (Table 1). 18S is highly conserved within the taxa considered here. T-Coffee was able to align all 18S sequences unambiguously over broad stretches, but two problematic regions remained. The inferred secondary structure of the *Agalma elegans* 18S molecule (Fig. 4a) localized these regions to the distal ends of helix B and helix 1399. Primary sequences for the problematic regions were found to fold similarly *in silico* across multiple taxa. This allowed for the identification of stems and loops and the alignment of homologous nucleotides.

Not only was the homology of nucleotides in the 16S alignment in question, the degree of variation meant that homology of secondary structure features in some regions was also unclear. The same secondary structure model (Fig. 4b) was applied to the entire matrix, so only the regions of the alignment that corresponded to secondary structure features shared by all taxa were improved by the methods used here. These were already the most conserved regions of the matrix, and the matrix aligned with the aid of secondary structure did not have any more included characters than preliminary alignments made without secondary structure information (not shown). Secondary structure information did, however, make it easier to improve the alignment within the regions that were already included. It was particularly helpful in refining regions adjacent to those that were so problematic that they had to be excluded. The program Circles reconstructed many features of the secondary structure of 16S from mutational covariance in the aligned matrix alone (not shown), indicating that homologous secondary structures had been successfully aligned for much of the gene. The concatenated alignment has been submitted to TreeBase (accession number M2247).

Phylogenetic Analyses and Hypothesis Testing

The degree of mutational saturation was assessed by plotting the number of observed nucleotide differences (the adjusted character distance of PAUP*) between each possible species pair against the corresponding number of inferred differences (the patristic distance of PAUP*). The presence of a plateau in this plot would indicate that the data are saturated for comparisons at some deeper nodes (Hassanin et al., 1998; Philippe and Forterre, 1999; Philippe et al., 1994). No such plateau was found. The

FIGURE 3. The distribution of collection localities. Each black dot indicates a site where at least one of the specimens used in this study was collected.

TABLE 1. A complete list of the specimens collected for this work. The abbreviation BW in the depth column designates specimens that were collected with blue-water SCUBA diving and are from depths of 0 to 30 m. Institution abbreviations are as follows: M = Monterey Bay Aquarium Research Institute, Moss Landing, CA; Y = Yale Peabody Museum (YPM), New Haven, CT; E = El Colegio de la Frontera Sur, Chetumal, Mexico. Catalog numbers are given for YPM specimens. In some cases the entire specimen has been used, and only photographs remain at the YPM.

Taxon	18S	16S	Voucher	Latitude	Longitude	Depth (m)
Abylopsis tetragona	AY937345	AY935303	Y 35350	39.75°N	70.87°W	BW
Agalma clausi	AY937312	AY935270	Y 35024	37.43°N	72.68°W	BW
Agalma elegans	AY937313	AY935271	Y 35029	37.63°N	73.45°W	BW
Agalma elegans	AY937340	AY935298	—	36.22°N	123.77°W	BW
Agalma okeni	AY937314	AY935272	Y 35030	38.17°N	72.98°W	BW
Apolemia sp. 1	AY937315	AY935273	Y 35035	38.48°N	73.00°W	BW
Apolemia sp. 2	AY937330	AY935289	Y 35089	36.21°N	122.53°W	1550
Apolemia sp. 3	AY937331	AY935290	Y 35090	36.23°N	122.77°W	387
Apolemia sp. 4	AY937332	AY935291	Y 35091	36.22°N	123.77°W	1155
Athorybia rosacea	AY937316	AY935274	Y 35031	38.91°N	70.27°W	BW
Athorybia rosacea	AY937352	AY935310	Y 35356	24.32°N	109.20°W	BW
Bargmannia amoena	AY937333	AY935292	M	36.36°N	122.66°W	1364
Bargmannia elongata	AY937334	—	M	36.22°N	123.77°W	877
Bargmannia elongata	—	AY935321	Y 35364	36.33°N	122.9°W	918
Chelophyes appendiculata	AY937346	AY935304	Y 35049	39.7°N	70.90°W	BW
Chuniphyes multidentata	AY937335	AY935293	M, Y 35348	36.21°N	122.53°W	661
Clausophyes ovata	AY937336	AY935294	M, Y 35349	36.21°N	122.53°W	2000
Clausophyid sp. 1	AY937347	AY935305	Y 35351	36.57°N	122.52°W	3800
Cordagalma cordiforme	AY937317	AY935275	Y 35032	37.68°N	73.13°W	BW
Craseoa lathetica	AY937339	AY935297	Y 35044	36.23°N	122.77°W	402
Diphyes dispar	AY937318	AY935276	Y 35033	36.98°N	73.85°W	BW
Erenna sp.	AY937361	AY935319	Y 35362	24.32°N	109.2°W	910
Forskalia asymmetrica	AY937319	AY935277	Y 35034	40.31°N	68.13°W	610
Forskalia edwardsi	AY937320	AY935278	Y 35036	37.84°N	73.83°W	BW
Forskalia edwardsi	AY937354	AY935312	E	25.45°N	109.84°W	BW
Forskalia edwardsi	AY937355	AY935313	E	25.45°N	109.84°W	BW
Forskalia formosa	AY937344	AY935302	Y 35048	39.75°N	70.87°W	BW
Forskalia tholoides	AY937321	AY935279	Y 35037	36.97°N	74.00°W	BW
Gymnopraia lapislazula	AY937359	AY935317	Y 35360	36.70°N	122.04°W	420
Halistemma rubrum	AY937323	AY935281	Y 35038	43.68°N	7.33°E	BW
Halistemma rubrum	AY937325	AY935283	Y 35040	38.85°N	72.45°W	BW
Halistemma rubrum	AY937358	AY935316	E, Y 35359	23.62°N	108.78°W	363
Hippopodius hippopus	AY937341	AY935299	Y 35045	39.70°N	70.92°W	BW
Hippopodius hippopus	AY937356	AY935314	E	24.32°N	109.20°W	BW
Lensia conoidea	AY937360	AY935318	Y 35361	36.72°N	122.07°W	350
Muggiaea atlantica	AY937337	AY935295	—	36.22°N	123.77°W	BW
Nanomia bijuga	AY937324	AY935282	Y 35039	37.45°N	74.02°W	BW
Nanomia bijuga	AY937338	AY935296	Y 35043	36.22°N	123.77°W	BW
Nectadamas diomedeae	AY937348	AY935306	Y 35352	36.70°N	122.05°W	392
Nectopyramis natans	AY937349	AY935307	Y 35353	36.57°N	122.52°W	759
Physalia physalis	—	AY935284	Y 35345	39.15°N	72.4°W	0
Physophora hydrostatica	AY937342	AY935300	Y 35046	39.75°N	70.60°W	BW
Praya dubia	AY937326	AY935285	Y 35346	36.71°N	122.05°W	298
Rhizophysa eysenhardti	AY937351	AY935309	Y 35355	24.32°N	109.20°W	BW
Rhizophysa filiformis	AY937327	AY935286	Y 35347	40.31°N	68.14°W	BW
Rosacea flaccida	AY937328	AY935287	Y 35041	38.9°N	70.27°W	BW
Sphaeronectes gracilis	AY937343	AY935301	Y 35047	39.57°N	71.40°W	BW
Stephalia dilata	AY937357	AY935315	Y 35358	24.31°N	109.20°W	1349
Stephanomia amphytridis	AY937322	AY935280	Y 35076	40.31°N	68.13°W	800
Sulculeolaria quadrivalvis	AY937353	AY935311	Y 35357	25.45°N	109.84°W	BW
Sulculeolaria quadrivalvis	AY937329	AY935288	Y 35042	38.48°N	73.03°W	BW
Vogtia glabra	AY937350	AY935308	Y 35354	40.31°N	68.14°W	700
Vogtia pentacantha	AY937362	AY935320	Y 35363	36.7°N	122.05°W	617
Porpita porpita	—	AY935322	—	24.32°N	109.2°W	0–100
Velella velella	—	AY935323	—	36.60°N	123.77°W	0

same molecular evolution models were selected, with only minor effects on parameter estimates, whether or not the outgroup was included. The parameter values estimated from the runs with the outgroup excluded were used in the likelihood analyses (Table 2). A burn-in of 100,000 generations was found to be sufficient, and was used for all Bayesian analyses. Table 3 summarizes the results of the ML and MP heuristic searches. 16S consistently gave better resolution at the tips of the trees, and 18S gave better resolution at deeper nodes in the trees. The best trees found by MP heuristic searches of the 16S data differed from each other in the relationships within the group containing *Agalma* and *Athorybia*, and in the position of *Bargmannia* and *Apolemia*, but were similar in

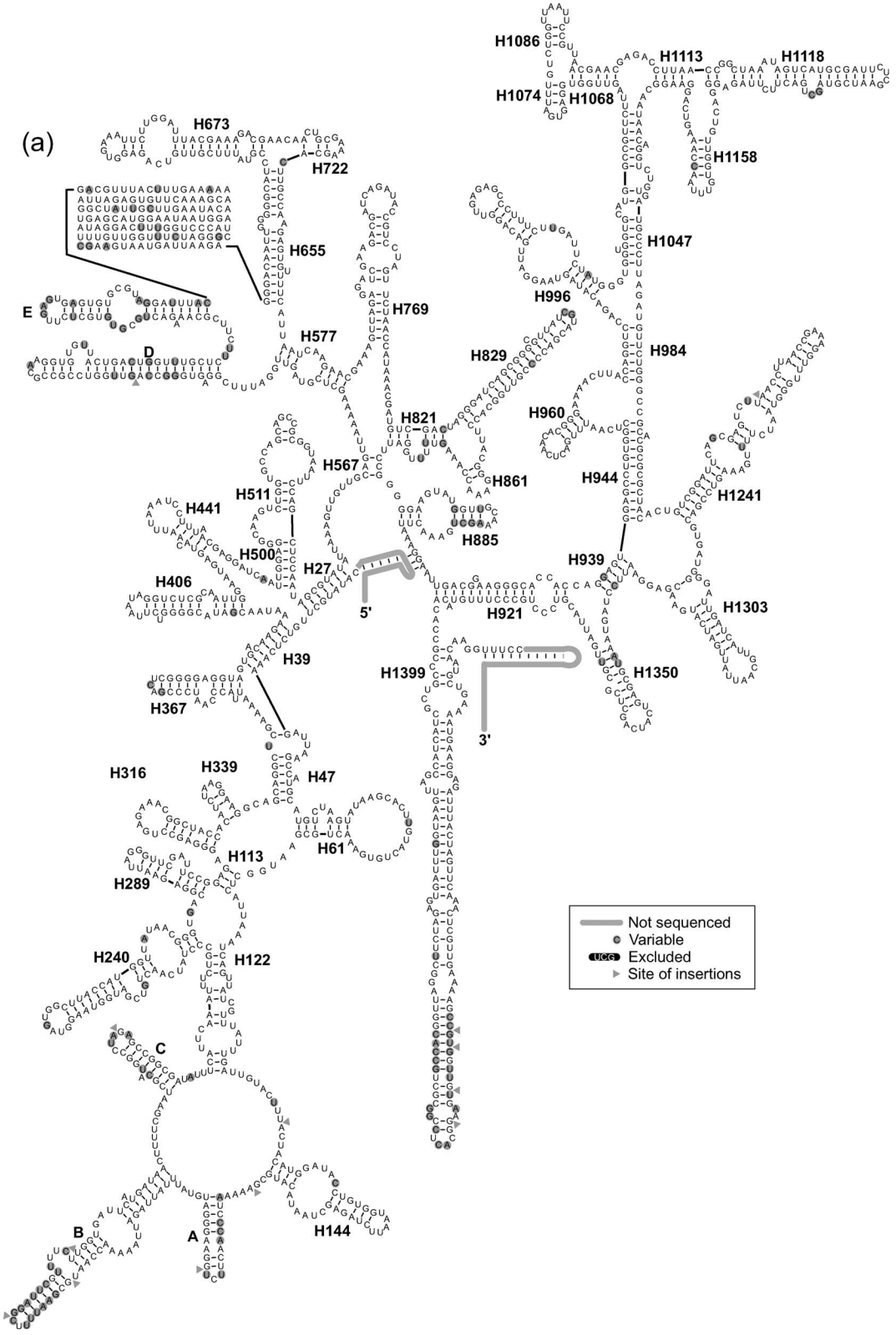

FIGURE 4. The estimated secondary structure of the sequenced rRNA regions mapped onto the *Agalma elegans* sequences. (a) 18S, complete molecule. (b) 16S, domains IV and V. Gray circles behind nucleotides indicate sites that are variable within siphonophores. Inverted nucleotides (white on black) indicate regions that were excluded from the phylogenetic analyses. Light gray lines indicate regions of the molecule that were not sequenced. Triangles indicate sites were some taxa have insertions. Helix numbering corresponds to the *Escherichia coli* structural models at the Comparative RNA website (Cannone et al., 2002). Helixes that do not have clear homologs to the helixes of the *E. coli* structural models have been lettered consecutively. *(Continued)*

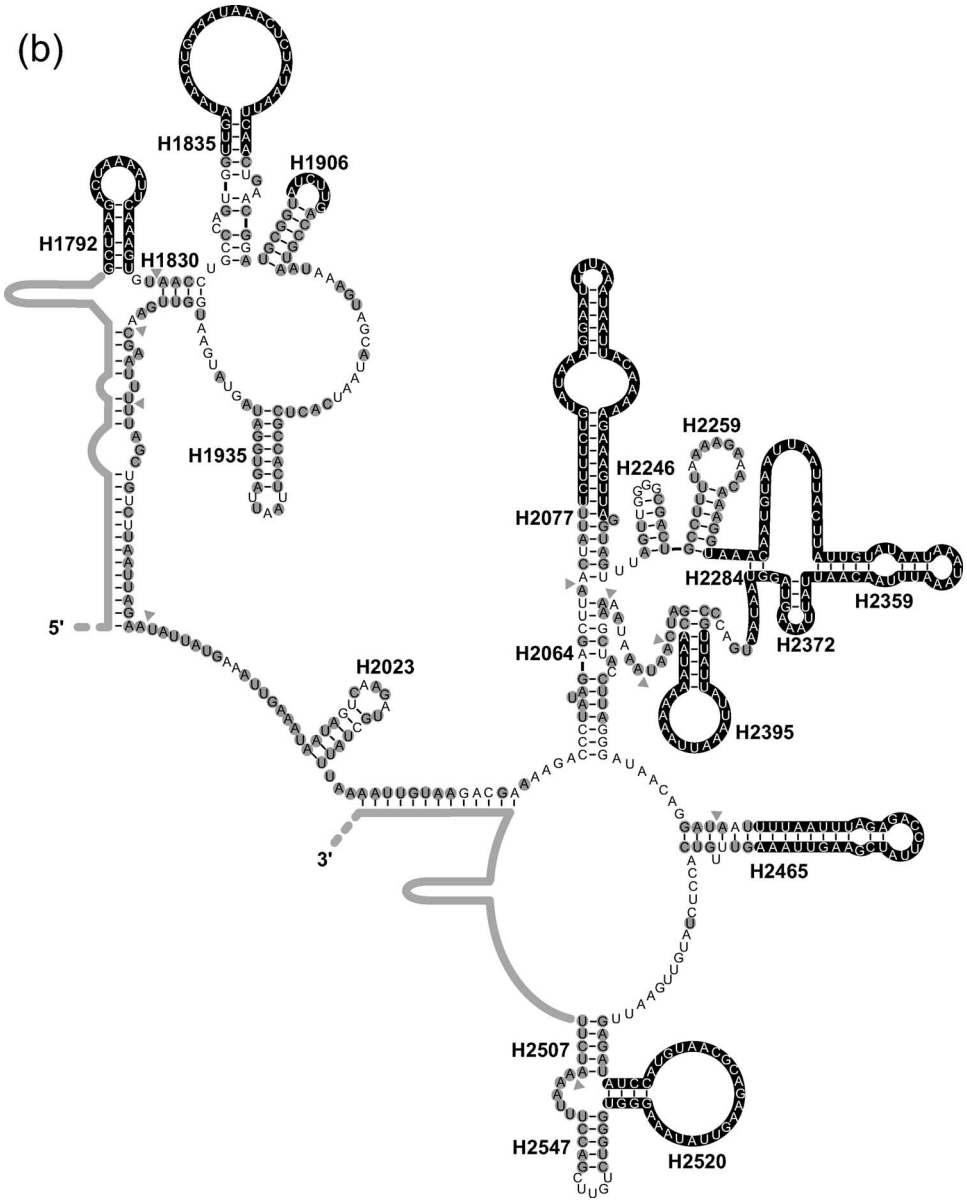

FIGURE 4. (Continued)

most other respects. The trees found in the MP heuristic searches of the 18S data set differed in the position of *Nanomia bijuga* and the basal relationships within the calycophorans, but were otherwise similar. The branch lengths of some calycophorans were much longer than those of other taxa in the 16S analyses, but not in the 18S analyses (Fig. 5). This was particularly pronounced in the hippopodiids and diphyomorphs.

The ILD test rejected the hypothesis that the 16S and 18S data sets were congruent ($p = 0.02$). *Cordagalma cordiforme*, a physonect, was found to be responsible for much of the incongruence. When it was temporarily excluded the ILD test found no significant conflict ($p = 0.52$). *C. cordiforme* was placed within the Calycophorae as sister to the hippopodiids in all 16S analyses (99% MP bootstrap, 68% ML bootstrap, and 68% posterior probability). All 18S analyses placed it outside of the Calycophorae (with support values for a monophyletic Calycophorae of 91% MP bootstrap, 86% ML bootstrap, and 100% posterior probability).

The topologies of the analyses of the combined data were largely consistent (Fig. 6), with the notable exception of the placement of *Cordagalma cordiforme*. MP analysis of the combined data set placed *C. cordiforme* as sister to the hippopodiids (91% MP bootstrap), whereas Bayesian analysis recovered a monophyletic Calycophorae (100% posterior probability). ML analyses of the combined data recovered a monophyletic Calycophorae, but bootstrap support was low (57%). *C. cordiforme* has the longest branch of all physonects in the

TABLE 2. Summary of sequencing, alignment, and model selection results. Molecular models were unlinked in the Bayesian analysis of the combined data, so there was no separate model for the combined data set.

	18S	16S	Combined
PCR product length	1751–1760	508–697	—
Included characters	1776	348	2124
Variable characters	206	227	433
Parsimony-informative characters	113	202	315
ModelTest model	TrN+I+Γ	TVM+I+Γ	TVM+I+Γ
MrModelTest model	GTR+I+Γ	GTR+I+Γ	—

16S and combined analyses. It did not have any rearrangements of secondary structure, or major insertions or deletions, within the region of 16S rRNA considered here. Because the hippopodiids usually have the longest branches of the calycophorans in these same analyses, it appears that the inclusion of *C. cordiforme* within the calycophorans in analyses that include 16S could be an artifact of long-branch attraction. *C. cordiforme* does not share any calycophoran morphological synapomorphies.

The SOWH test rejected all topological null hypotheses (Table 4).

Morphological Observations and Character Evolution

The morphological character matrix is available in the online supplemental materials. Monoecy versus dioecy (Fig. 7), the presence/absence of a descending pallial canal, and the orientation of the nectosome relative to the siphosome were scored, when possible, and traced on the phylogeny using parsimony. The relevance of these characters is addressed in the Discussion section.

Parsimony analyses of the gain and loss of zooid types suggested that nectosomal nectophores arose once, were lost at least once, and differentiated from one to two types at least once (Fig. 8a). They also indicate at least two reductions from two types of nectosomal nectophores to one type. Palpons were lost one to two times (Fig. 8b). Bracts originated once and were then lost one to three times (Fig. 8c). There were from one to four transitions from one type of bract to two types, and one transition to four types. All siphonophores have at least one type of gastrozooid. Beyond this, *Physalia physalis* has three types, *Stephalia dilata* has two, and *Bargmannia elongata* has two. Parsimony reconstruction of the history of gastrozooid evolution is consistent with one transition from one to three types of gastrozooids, and one or two transitions to two types (not shown).

TABLE 3. Summary of phylogenetic inferences results. The score of the MP searches is the number of steps; the score of the ML searches is the log likelihood.

Criterion	Gene	Best score	Number of unique trees with best score	Fraction of runs that found a tree with the best score
MP	16S	1174	41	0.18
MP	18S	375	1152	1.00
MP	Combined	1578	144	0.98
ML	16S	−5519.9	1	0.18
ML	18S	−4730.0	1	0.98
ML	Combined	−11015.6	1	1.00

TABLE 4. Topological constraints assessed with the SOWH parametric bootstrap test. D is the difference in parsimony score between the best tree overall and the best tree constrained to be consistent with the hypothesized topology. The fraction of D values from one hundred simulated datasets that were greater than the observed D value is indicated by p. A $p < 0.05$ indicates a significant D and leads to the rejection of the hypothesized constraint. Some analyses included (+) or excluded (−) particular taxa.

Constraint (monophyly)	D	p
Brachystelia	30	<0.01
Physonectae	15	<0.01
Physonectae − *C. cordiforme*	5	0.03
Agalmatidae	19	<0.01
Agalmatidae *sensu stricto* + *C. cordiforme*	14	<0.01
Agalmatidae *sensu stricto* + *S. amphytridis*	8	0.02
Agalmatidae *sensu stricto* + *Bargmannia*	12	<0.01
Diphyomorphs −*Sphaeronectes*	19	<0.01
Prayomorphs	15	<0.01
Prayomorphs + *C. cordiforme*	5	0.02

The likelihood-ratio test comparing the one–transition rate ($\alpha = \beta$) versus the two-rate (α, β) model for the gain and loss of zooids rejected the one-rate null hypothesis at the 95% confidence level only for gastrozooids (Table 5). The tests were significant at the 90% confidence level for palpons and bracts and not significant for nectophores. ML estimated $\beta > \alpha$ for all zooid types in the two–transition rate analyses. The means of the Bayesian posterior distributions of α and β were greater than the corresponding ML estimates in all cases, and the mean of β was always greater than the mean of α (Table 5; Fig. 9).

DISCUSSION

The Phylogeny of the Siphonophores

The phylogeny inferred here (Fig. 6), which includes 52 siphonophores, is consistent with an earlier analysis of the Hydrozoa that included 9 siphonophores (Collins, 2002). The ability to sample more taxa through the use of blue-water diving and ROVs, as well as the addition of another gene, has further clarified the relationships between the major groups of siphonophores and provided finer scale resolution within them. The monophyly of the Cystonectae was strongly supported. The position of the root indicated that the Cystonectae are sister to all other siphonophores. We call this other clade, which includes the historically recognized Physonectae and Calycophorae, the Codonophora. This is Greek for "bell-bearer," a reference to the nectosome apomorphy that defines this group. Within the Codonophora, the physonects are found to be paraphyletic and to give rise to the Calycophorae (Fig. 6; Table 4). There is strong support for the monophyly of *Apolemia*, which the 18S and combined data suggest is sister to all other Codonophora. There is little resolution at the base of the sister group to *Apolemia* in all analyses.

Bayesian analyses strongly support the monophyly of the Calycophorae, though ML support is low and MP analyses of 16S appear to be subject to the long-branch

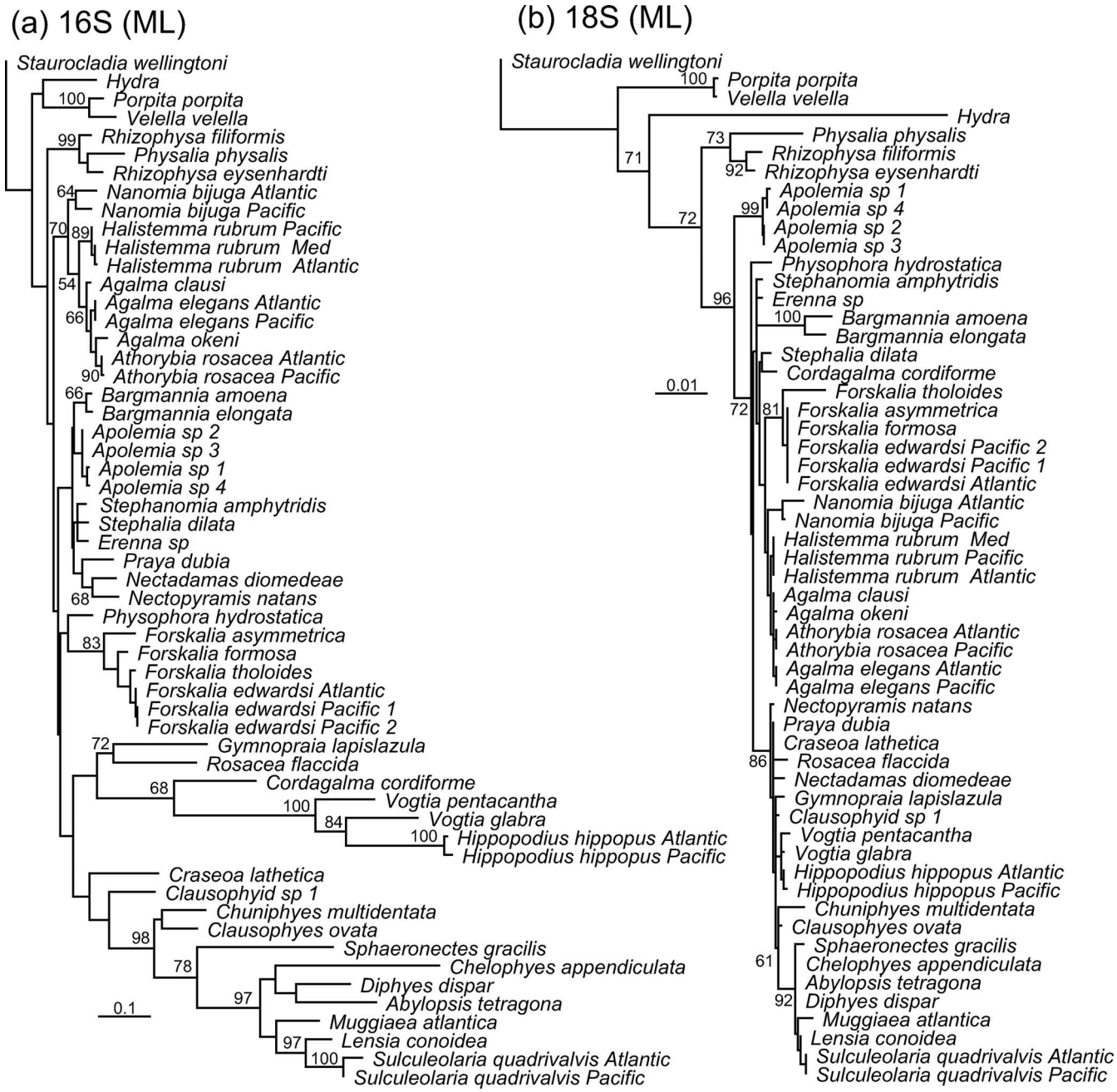

FIGURE 5. Phylograms depicting the structure of the best trees found in 50 ML heuristic searches of (a) the 16S data set (under a TVM+I+Γ model) and (b) the 18S data set (under a TrN+I+Γ model). ML bootstrap scores greater than 50% are shown where space permits (estimated from 100 bootstrap replicates).

attraction problems with the physonect *Cordagalma cordiforme*. If this taxon is excluded from the analysis, the MP bootstrap support for a monophyletic Calycophorae is 86% (not shown). The Calycophorae have often been divided into two broad groups, which we refer to as the prayomorphs and the diphyomorphs after Mackie et al. (1987). Our data indicate that the prayomorphs are paraphyletic and give rise to the diphyomorphs (Fig. 6; Table 4).

The molecular data indicate that *Hippopodius hippopus* is nested within *Vogtia*. The name *Hippopodius* Quoy & Gaimard 1827 has precedence over *Vogtia* Kölliker 1853, so a nomenclatural revision would require that the four valid taxa currently known as *Vogtia* be changed to *Hippopodius*. We defer a decision about this name change until more is known about the two *Vogtia* species that are not included here. *Sphaeronectes* is a group of several calycophoran species that retain larval characters into

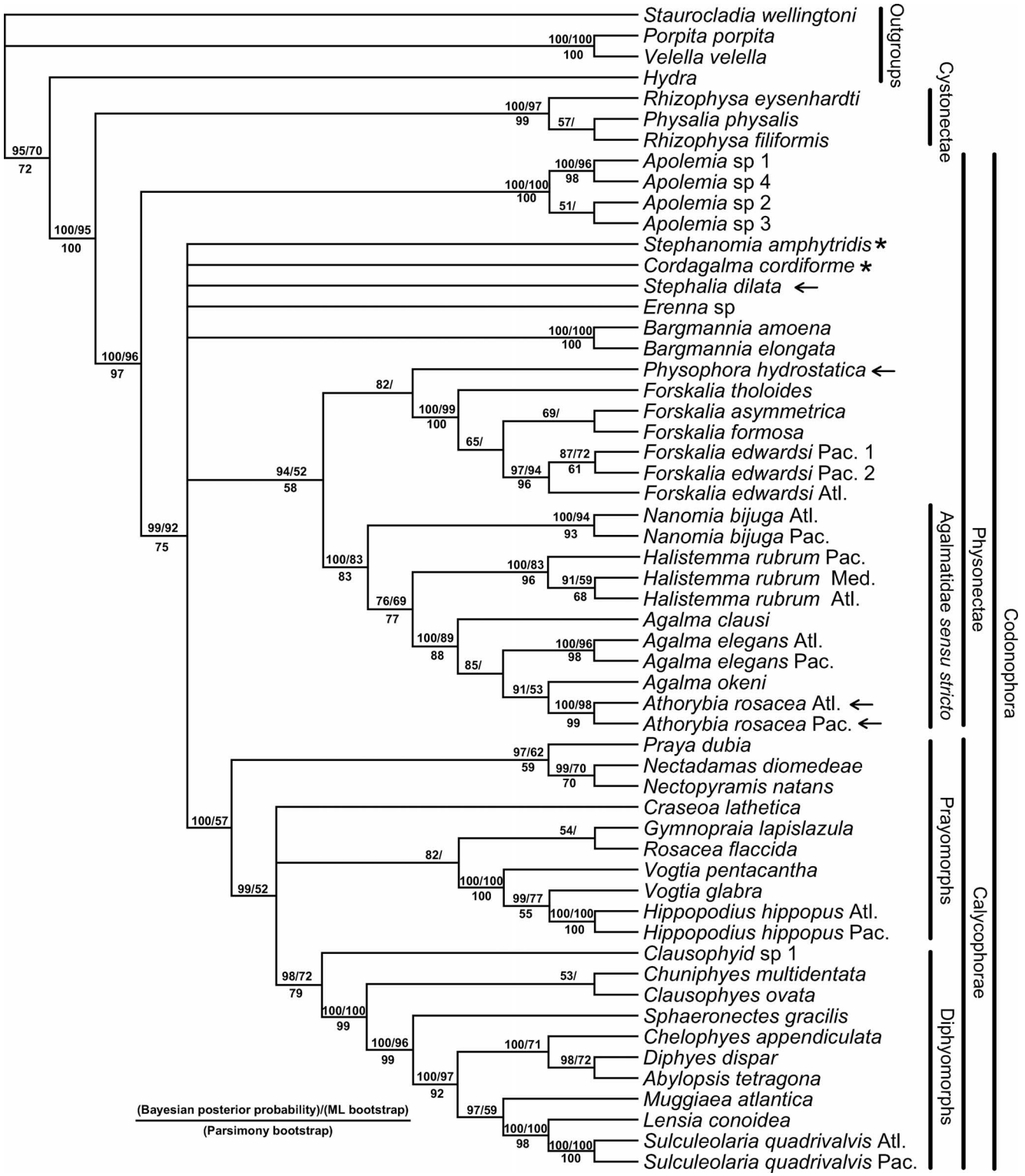

FIGURE 6. Consensus tree of all post burn-in trees for the Bayesian analysis of the combined data set (from an initial set of 20 million trees). The left score above the branch is the Bayesian posterior probability (%), the right score above the branch is the ML bootstrap support value (%), and the score below the branch is the MP bootstrap support value (%). The bars to the right of the species names indicate clades and grade taxa. Asterisks indicate species that are traditionally grouped within the Agalmatidae, but do not fall within the Agalmatidae *sensu stricto*. Arrows indicate short-stemmed physonects, which have often been considered to form a group called the Brachystelia. Atl., Atlantic; Med., Mediterranean; Pac., Pacific.

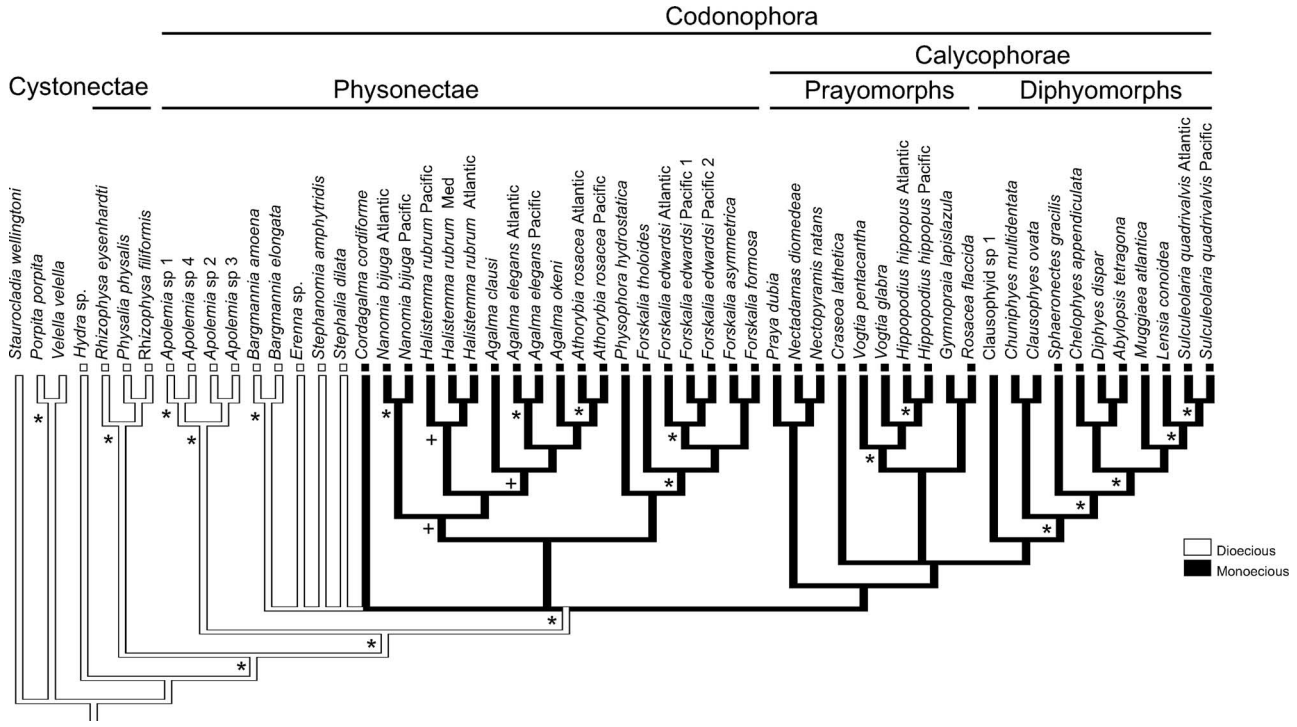

FIGURE 7. Parsimony ancestral character state reconstructions for monoecy versus dioecy (white, dioecious; black, monoecious). Asterisks indicate nodes that have MP bootstrap, ML bootstrap, and Bayesian posterior probabilities all greater than 90%. Crosses indicate nodes for which all support values are greater than 80%. The boxes next to taxon names indicate the observed character states, when known.

adulthood. It has been placed with the prayomorphs by some authors (Leloup, 1954; Stepanjants, 1967; Totton, 1954) and within the diphyomorphs by others (Totton, 1965). The present study has found *Sphaeronectes gracilis* to be within the diphyomorphs. The Diphyidae (represented here by *Diphyes dispar*, *Sulculeolaria quadrivalvis*, *Lensia conoidea*, *Muggiaea atlantica*, and *Chelophyes appendiculata*) are paraphyletic and give rise to the Abylidae (represented by *Abylopsis tetragona*).

Determining how the siphonophores are related to the other hydrozoa would add much to our understanding of the origin of the extreme functional specialization of zooids within siphonophore colonies. In previous work, 18S alone was not sufficient to clearly resolve the relationship of siphonophores to other hydrozoans (Collins, 2002). The present study found 16S was only informative for inferring relationships between closely related siphonophores, so it is unlikely that it will be useful at this broader phylogenetic scale. Better sampling of a diversity of hydrozoan taxa and the use of additional molecular characters will be required to clarify these relationships.

Implications for the Evolution of Gross Morphology

The origins of short-stemmed Codonophora.—Although most siphonophores have a long stem with linearly organized siphosomal zooids, some have a bulb-shaped siphosome that bears the siphosomal elements in whorls or separate rows. These short-stemmed physonects have often been considered a natural group known as the Brachystelia (Haeckel, 1888). We have included three species in the present study, *Stephalia dilata*, *Athorybia rosacea*, and *Physophora hydrostatica* (Fig. 1e to g), that represent all three Brachystelia groups (the Rhodaliidae, Athorybiidae, and Physophoridae, respectively). Our data indicate that these taxa do not form a natural group (Fig. 6; Table 4), and that the short-stemmed morphology has evolved multiple times within the Codonophora. A recently improved understanding of morphological data is consistent with this conclusion. Though their colony form is superficially similar, the organizations of zooids in the siphosome of the three groups of short-stemmed Codonophora (Bigelow, 1911; Pugh, 1983, 2005) are very different.

Athorybiid species bear a striking resemblance to the larvae of *Agalma* species, suggesting that they may have arisen from *Agalma* by paedomorphosis (Fewkes, 1880; Schneider, 1896). Our data, which indicate that *Athorybia* is nested within *Agalma*, are consistent with this hypothesis. We have chosen not to change the name of *Athorybia* until further morphological or molecular data can clarify the implications for the other two species of Athorybiidae not included in the present analysis.

Monoecy versus dioecy.—Each gonophore (reproductive medusa) is of a single sex. Although some siphonophore colonies are monoecious, bearing gonophores of both sexes, others are dioecious and have separate male and female colonies. The most-parsimonious explanation for the history of sexual specialization is that the common

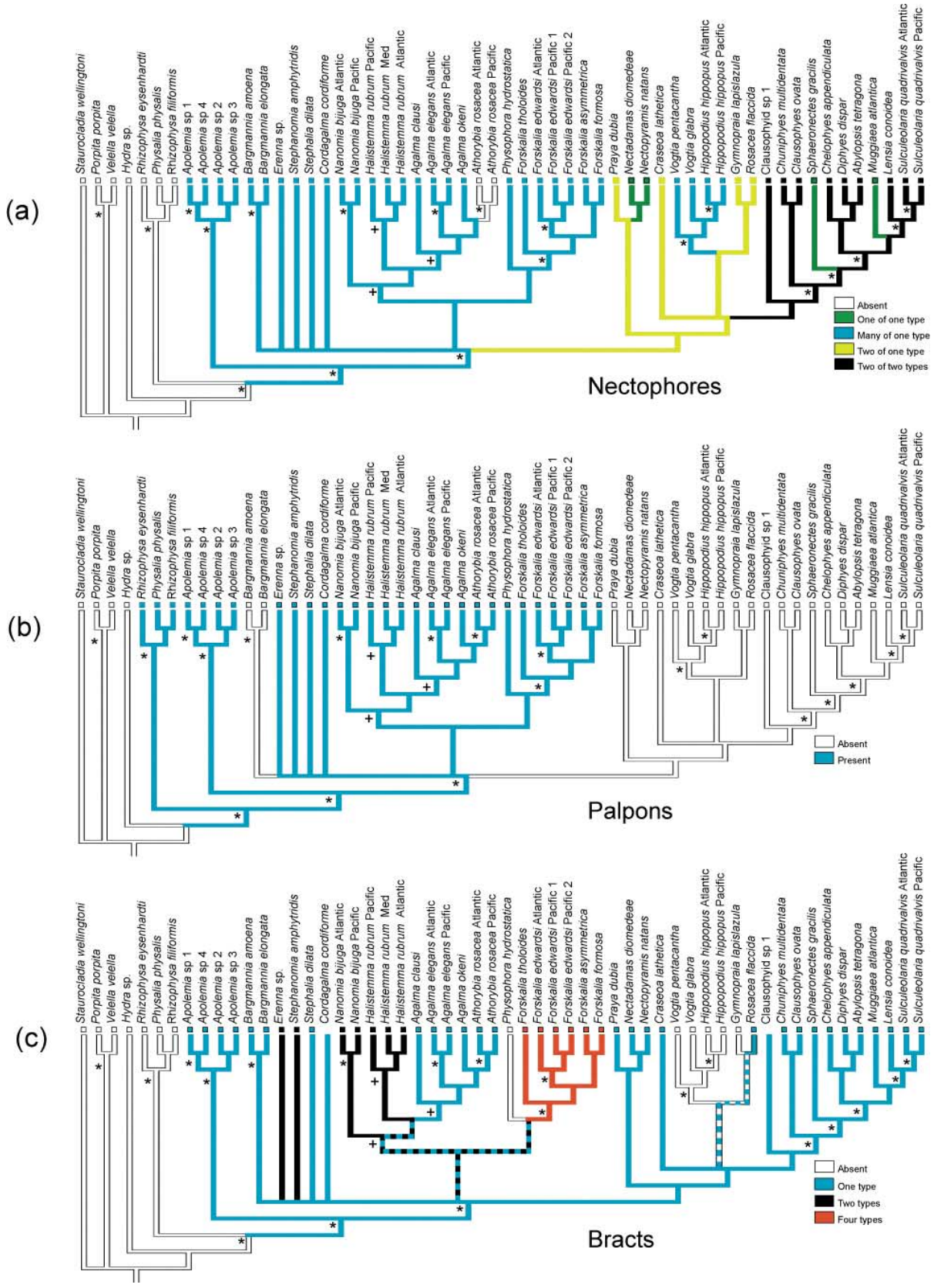

FIGURE 8. Parsimony ancestral character state reconstructions for zooid types. (a) Nectophores. (b) Palpons. (c) Bracts. Asterisks indicate nodes that have MP bootstrap, ML bootstrap, and Bayesian posterior probabilities all greater than 90%. Crosses indicate nodes for which all support values are greater than 80%. The boxes next to taxon names indicate the observed character states, when known.

TABLE 5. Summary of results of ML and Bayesian analyses of the gain and loss of zooid types. Mean values ± standard deviations are shown. ML statistics were compiled across all trees in the posterior distribution. α is the transition rate for the gain of zooid types, β is the transition rate for the loss of zooid types. H_0 is the one transition rate model ($\alpha = \beta$), H_1 is the two transition rate model (α and β not constrained to each other).

	Nectophores	Gastrozooids	Palpons	Bracts
Maximum likelihood				
ln(likelihood H_0)	-21.22 ± 0.61	-15.09 ± 0.49	-10.53 ± 1.03	-32.98 ± 1.41
Rate ($\alpha = \beta$)	2.31 ± 0.16	1.28 ± 0.09	1.92 ± 0.40	2.72 ± 0.29
ln(likelihood H_1)	-21.17 ± 0.62	-11.99 ± 0.09	-8.77 ± 1.50	-31.14 ± 1.34
α	1.84 ± 0.23	7.25 ± 1.84	0.28 ± 0.54	1.19 ± 0.23
β	2.54 ± 0.20	206.14 ± 52.59	4.93 ± 0.57	6.04 ± 0.97
p	0.74	0.013	0.061	0.055
Bayesian				
Prior ($\alpha = \beta$)	2.86 ± 1.26	1.74 ± 0.91	2.69 ± 1.62	3.16 ± 1.15
α	2.50 ± 0.79	27.96 ± 18.34	1.04 ± 1.35	2.50 ± 0.66
β	3.30 ± 1.62	641.40 ± 258.01	6.14 ± 4.22	6.76 ± 3.03

ancestor of siphonophores was dioecious (Fig. 7). The phylogeny is consistent with a single gain of monoecy within the Codonophora, but a lack of topological resolution makes it impossible at the present time to rule out the possibility that it arose more than once.

Nectophore canal system.—Nectophores are propulsive medusae that lack feeding and reproductive structures (Fig. 2e to f). The most conspicuous nectophores are the large swimming bells found along the nectosome of the Codonophora. Propulsive medusae are also found

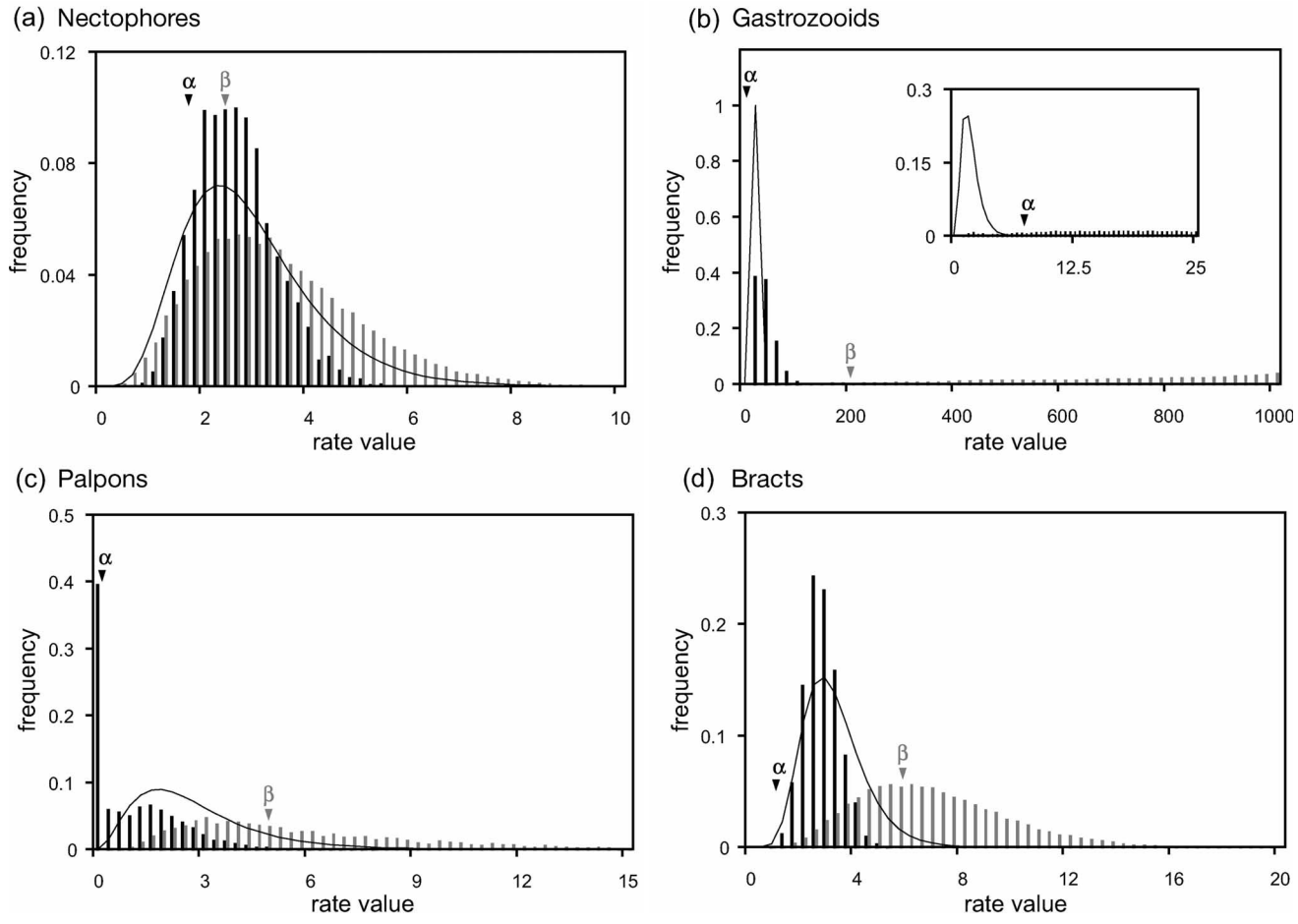

FIGURE 9. Histograms of the estimated Bayesian posterior probabilities for the transition rates for the increase (α, shown as black bars) and decrease (β, shown as gray bars) in the number of zooid types. The rates are shown on the ordinate axis. The same prior was used for both α and β. This prior was empirically derived from the one-rate ($\alpha = \beta$) likelihood surface (shown as a solid line, calculated at the same intervals as the histogram bins). The mean of the ML estimates of α and β made across the posterior sample of trees are shown with arrowheads on each histogram (these are not the same as the means of the posterior distributions of transition rates). The inset of panel b is a histogram across the lower-magnitude portion of the probability density distribution of the gastrozooid rates (note that the α distribution has become spread out because of the smaller bin size; the magnitude of β in this range is too small to be visible).

in the siphosome of cystonects and some calycophorans, where they are associated with the reproductive structures (Totton, 1965). These siphosomal nectophores can sometimes look quite similar to the medusae specialized for sexual reproduction, and it may be that propulsive medusae (which are not found to be retained in the colonies of any other hydrozoans) are derived from retained reproductive medusae. The siphosomal nectophores are not well understood, though, and too few data are available to make a survey of them. Only nectosomal nectophores, which are the best characterized of all siphonophore zooids, will be addressed in the present study.

The descending pallial canal is a feature of the gastrovascular system of nectophores that is present in some species, but absent in others. We have scored the presence of the descending pallial canal in all physonects, except *Athorybia rosacea*, which lacks nectophores. This character was not scored for calycophorans because of difficulties imposed by the derived nature of their nectophores (see Haddock et al., 2005, for a discussion of nectophore canal systems). A descending pallial canal is present in all of the monoecious physonects and is absent in the dioecious physonects. Monoecy/dioecy and presense/absense of the descending pallial canal are therefore consistent in the groupings they suggest within the Codonophora. As nectophores and sexual gonophores are both medusae, and presumably share many features of development, these two characters may have pleiotropic links.

The orientation of the nectosome relative to the siphosome.—The siphosomal elements of long-stemmed siphonophores are all located in a single line along one side of the stem, which, by convention, is taken to be ventral (Haeckel, 1888). The nectophores of species belonging to the grade Physonectae are likewise attached in a line along one side of the stem, although twisting of the stem and bending of the lamellae joining the nectophores to the stem leads to biserial or whorled arrangements. Whether the nectophores are located on the same side of the stem as the siphosomal elements (i.e., ventral) or on the opposite side (i.e., dorsal) has been addressed only rarely, and the topic has been confused by many false assumptions (Garstang, 1946; Haeckel, 1888:189; Totton, 1965). The nectosomal growth zones of calycophorans are not understood well enough at this time to assign them a simple dorsal or ventral position.

We examined preserved material from all of the physonects included in the phylogeny to determine the orientation of the nectosome relative to the siphosome. The nectophores were found to be attached dorsally in two clades, each of which has good phylogenetic support. The first group consists of *Bargmannia elongata* and *B. amoena*, and has a Bayesian posterior probability of 100% and MP and ML bootstrap support values of 100%. The second group includes *Nanomia bijuga*, *Halistemma rubrum*, *Agalma clausi*, *A. elegans*, and *A. okeni*, all of which have historically been placed in the Agalmatidae. Together with *Athorybia rosacea*, which has lost its nectophores and cannot be scored for this character, this second group has a Bayesian posterior probability of 100% and MP and ML bootstrap support values of 83%. We call this second group the Agalmatidae *sensu stricto* (Fig. 6). The SOWH test rejects the hypothesis that *Bargmannia* and the Agalmatidae *sensu stricto* form a monophyletic clade (Table 4).

Two taxa, *Cordagalma cordiforme* and *Stephanomia amphytridis*, possess a ventral nectosome and did not form a group with the Agalmatidae *sensu stricto* in analyses of the molecular data (Fig. 6; Table 4). They have, however, traditionally been placed in the Agalmatidae. Our results therefore support the view that the Agalmatidae is merely a catch-all group for a variety of unrelated physonects (Pugh, 1998).

The Gain and Loss of Zooid Types

Understanding the evolution of the division of labor is key to understanding the origin and diversification of complexity in biological systems. Functional specialization between repeated units occurs at all levels of biological organization and may be governed by similar evolutionary mechanisms in each case. Functional specialization between duplicated genes is thought to play a major role in innovation at the genomic level (e.g., Force et al., 1999). It is widely recognized that understanding the origins and evolution of functional specialization between cells is central to understanding the transition from unicellular life to multicellular organisms (e.g., Buss, 1987).

Although there is a rich tradition of the study of the division of labor in eusocial insects (Wilson, 2000), there have been few investigations of the same phenomenon in colonial animals. Little is even known about the developmental mechanisms that lead to the differentiation of specialized zooids (Cartwright et al., 1999; Harvell, 1994). The most detailed previous study of the evolution of functional specialization in colonial animals focused on the cyclostome bryozoans (McShea and Venit, 2002). McShea and Venit scored three skeletal characters related to the functional specialization and used several methods to look for evolutionary bias. Although the results were not conclusive, they did suggest that there was no bias towards an increase in functional zooid organization and colonial integration.

Siphonophores have a greater division of labor and more precise organization of specialized zooids than any other extant colonial animals (Beklemishev, 1969). These properties make siphonophores particularly well suited for investigations of the division of labor. There are, however, several technical limitations that preempt a comprehensive analysis of the gain and loss of all zooid types across the taxa included in the present analysis. The primary problem is that the zooid inventories of many rare and fragile taxa are simply not known. We have therefore considered only the best described categories of zooids. We have also only scored mature zooids found in adult colonies, as too little is known about ontogenetic shifts in zooid morphology and colony maturation to include earlier stages of development. It is important to explicitly

note two potential sources of error in the maximum likelihood and Bayesian methods used here to investigate the morphological data. First, we have used molecular branch lengths as estimates of the true branch lengths, even though our data are not clock-like (not shown). Second, these methods assume that the character change is at equilibrium. As with similar previous studies (e.g., Pagel et al., 2004), this has not been tested. It is not yet clear how large of an impact these potential sources of error have on the application of these methods.

Nectosomal nectophores.—Cystonects have no nectosome. All physonects, with the exception of *Athorybia* (which has lost its nectophores), have multiple nectophores of one type. Mature calycophoran colonies can have a single nectophore, two nectophores of one type, two nectophores of two types, or four or more nectophores of one type. In cases where there are two nectophores of a single type, they are arranged so that they are apposed to each other. In the cases where there are two nectophores of two types, they are displaced so that one is in front of the other. There are sometimes minor differences between apposed nectophores, but they are not nearly as dramatic as in cases where the two nectophores are displaced.

Parsimony character reconstruction suggests that the origin of the nectosome resulted in multiple nectophores of one type (Fig. 8a). Nectophores were then lost entirely in *Athorybia*. There was one shift to two nectophores of two types in Diphyomorphs, followed by two subsequent reductions to one nectophore of one type in *Sphaeronectes gracilis* and *Muggiaea atlantica*. The fact that these two species develop a single nectophore in different ways supports this inferred homoplasy. All calycophoran colonies develop a single larval nectophore. Definitive nectophores can arise later in development, and the larval nectophore is either shed or retained. *Sphaeronectes gracilis* does not develop definitive nectophores and retains its single larval nectophore throughout its life (Carré, 1969). *Muggiaea atlantica*, as inferred from work on a congener (Carré and Carré, 1991), develops a single definitive nectophore but then sheds its larval nectophore. Two other calycophorans in the present study, *Nectadamas diomedeae* and *Nectopyramis natans*, both develop a single mature nectophore in the same way that *M. atlantica* does (Pugh, 1992).

The hippopodiids (*Hippopodius* + *Vogtia*), like the physonects, have multiple nectophores of one type. However, their development differs fundamentally from the physonects. They first develop and then shed a typical calycophoran larval nectophore (Metschnikoff, 1874). Nectophore addition in the hippopodiids then occurs in the opposite direction to that in the physonects, such that the youngest nectophore is adjacent to the siphosome rather than furthest from it. Together these independent lines of phylogenetic and developmental evidence indicate that the hippopodiids have secondarily derived the physonect-like nectophore condition of having more than two nectophores of the same type.

The likelihood-ratio test did not reject the hypothesis that the one rate model explained the data as well as the two-rate model (Table 5). The posterior distributions of α and β were similar to each other and to the likelihood surface for the one-rate model that was used as the prior (Fig. 9a).

Gastrozooids.—Gastrozooids are polyps specialized for feeding. Most described species have only one type of gastrozooid, which arise directly in the growth zone at the anterior end of the siphosome. Every 7th to 10th gastrozooid of *Bargmannia elongata* grows larger and more darkly pigmented than the others as it matures, so that there are two types at maturity (Dunn, 2005). Gastrozooids arise outside the growth zone in at least two taxa, and in both cases there are at least two types. In *Physalia physalis* there are a total of three types of gastrozooids (Totton, 1960:328). The rhodaliids, represented in this study by *Stephalia dilata*, have two types of gastrozooids: one type lacks a tentacle but has well developed digestive structures, and the other type has a tentacle but has not been observed to ingest prey (Hissmann, 2005). This is perhaps the clearest case of subfunctionalization within siphonophores.

Parsimony analyses recovered two to three independent increases in the number of gastrozooid types and no reductions (not shown). The likelihood-ratio test rejected the hypothesis that the one-rate model fit the data as well as the two-rate model for gastrozooids ($p < 0.05$), and ML recovered a β much larger than α (Table 5). The mean of the Bayesian posterior distributions of α and β are larger than their corresponding ML estimates, and β is essentially flat over a wide range of large values (Fig. 9b). This high β transition rate for a change that was not recovered in the parsimony analysis is not anomalous. The ML and Bayesian methods used here for inferring parameters of morphological evolution rely on continuous-time Markov models (Lewis, 2001; Pagel, 1994, 1997). The transition rates of these models are not simply a measure of changes in a given direction per unit time; they measure the rate of change from one state, should the system be in that state, to another state. If there are few taxa in a given state (e.g., having multiple types of gastrozooids), then the observed number of changes from that state to other states will be low even if the corresponding transition rates are high.

Palpons.—Palpons, like gastrozooids, are modified polyps, but they are usually smaller and less substantial. They cannot ingest prey and have been hypothesized to serve excretory and defensive functions (Mackie et al., 1987). We have chosen to score only the presence or absence of palpons because differentiation between palpons is poorly understood at present. Parsimony suggested that palpons were present in the common ancestor of siphonophores and lost one or two times (Fig. 8b). ML and Bayesian analyses indicated that the rate of palpon loss when they are present exceeded the rate at which they are gained when absent (Table 5; Fig. 9c).

Bracts.—Bracts are large shield-like gelatinous structures found in the siphosome of most Codonophora. They are completely absent in the cystonects. Bracts play an important role in defense. Many have patches of nematocysts (stinging capsules) and can emit bright

bioluminescence from special patches of cells (e.g., Pugh, 1998, 1999).

Gymnopraia lapislazula (Haddock et al., 2005) and the hippopodiids (Totton, 1965) lack bracts, and it is not known if Clausophyid sp. 1 has bracts or not. The other calycophorans included here each have one type of bract. The picture is more complex in physonects. *Physophora hydrostatica* lacks bracts at maturity, but still has a larval bract. This indicates that *P. hydrostatica* has not lost the ability to produce bracts altogether, and, in fact, a new species of *Physophora* has recently been described that possesses two types of adult bract (Pugh, 2005). Other physonects have from one to four distinct types of bracts.

The parsimony analysis suggested that bracts originated along the Codonophora stem and that there were several increases and decreases in the number of bract types within the group (Fig. 8c). The likelihood ratio test rejected the hypothesis that the one-rate model explained the data as well as the two-rate model, though only weakly (Table 5). Both ML and Bayesian estimates of the transition rate of bract loss are greater than the transition rate of bract gain (Fig. 9d).

Summary of zooid gain and loss.—Our findings indicate that there has been a complex history of functional specialization in siphonophores. Like a previous study of cyclostome bryozoans (McShea and Venit, 2002), we find no bias in favor of the gain of zooid types, and some evidence of a bias towards the loss of functionally specialized zooids. As phylogenies become available for more colonial taxa this may be found to be a general pattern. The same technological advances that made it possible to collect intact specimens for the present study also open the door to investigations of the developmental processes that differentiate functionally specialized zooids and organize them into specific patterns at the level of the colony (Dunn, 2005), and of how siphonophores interact with their environment (e.g., Hissmann, 2005). Together with the present phylogeny, these studies will help clarify how a diversity of functional specialization has been realized across these "superorganisms" and how evolution acts to shape the division of labor.

ACKNOWLEDGEMENTS

This work was supported by a mini-PEET grant from the Society for Systematic Biology, a National Science Foundation Graduate Research Fellowship, and a NSF Doctoral Dissertation Improvement Grant (DEB-0408014). Additional support was provided by the David and Lucile Packard Foundation and NSF grant no. DEB-9978131 A000 (the Hydrozoan PEET Grant, thanks to C. Cunningham). Special thanks to L. Madin for providing blue water dive opportunities, and to G. Wagner for his support and advice. We are also grateful for the specimens provided by M. Youngbluth, for assistance at Villefranche-Sur-Mer by C. Sardet and C. Carré, and to J. Godfrey for diving support. Thanks to E. Edwards and A. Caccone for insightful comments on this manuscript. Thanks also to S. Stearns for the use of his computational facilities, and to the crews of the ROV Ventana, ROV Tiburon, RV Western Flyer, RV Point Lobos, Johnson-Sea-Link II, and the RV Oceanus. The detailed suggestions of two reviewers significantly improved this manuscript. CWD is grateful to G. Mackie for the gift of his library of siphonophore monographs, which greatly facilitated the examination of the historical literature.

REFERENCES

Beklemishev, W. N. 1969. Principles of comparative anatomy. Volume I. Promorphology. Oliver and Boyd, Edinburgh.

Bigelow, H. B. 1911. The Siphonophorae. Mem. Mus. Comp. Zool. Harv. 38:173–401.

Biggs, D. C., P. R. Pugh, and C. Carré. 1978. *Rosacea flaccida* n. sp., a new species of siphonophore (Calycophorae Prayinae) from the North Atlantic Ocean. Beaufortia 27:207–218.

Buss, L. 1987. The evolution of individuality. Princeton University Press, Princeton, New Jersey.

Cannone, J. J., S. Subramanian, M. N. Schnare, J. R. Collett, L. M. D'Souza, Y. Du, B. Feng, N. Lin, L. V. Madabusi, K. M. Muller, N. Pande, Z. Shang, N. Yu, and R. R. Gutell. 2002. The comparative RNA web (CRW) site: An online database of comparative sequence and structure information for ribosomal, intron, and other RNAs. BMC Bioinformatics 3:2.

Carré, D. 1969. Etude du développement larvaire de *Sphaeronectes gracilis* (Claus 1873) et de *Sphaeronectes irregularis* (Claus 1873), Siphonophores Calycophores. Cah. Biol. Mar. 10:31–34.

Carré, C., and D. Carré. 1991. A complete life cycle of the calycophoran siphonophore *Muggiaea kochi* (Will) in the laboratory, under different temperature conditions: Ecological implications. Phil. Trans. R. Soc. Lond. B Biol. Sci. 334:27–32.

Cartwright, P., J. Bowsher, and L. W. Buss. 1999. Expression of a Hox gene, Cnox-2, and the division of labor in a colonial hydroid. Proc. Natl. Acad. Sci. USA 96:2183–2186.

Collins, A. G. 2000. Towards understanding the phylogenetic history of Hydrozoa: Hypothesis testing with 18S gene sequence data. Sci. Mar. 64:5–22.

Collins, A. G. 2002. Phylogeny of Medusozoa and the evolution of cnidarian life cycles. J. Evol. Biol. 15:418–432.

Cunningham, C., and L. Buss. 1993. Molecular evidence for multiple episodes of paedomorphosis in the family Hydractiniidae. Biochem. Syst. Ecol. 21:57–69.

De Rijk, P., and R. De Wachter. 1993. DCSE, an interactive tool for sequence alignment and secondary structure research. Comput. Appl. Biosci. 9:735–740.

De Rijk, P., J. Wuyts, and R. De Wachter. 2003. RnaViz 2: An improved representation of RNA secondary structure. Bioinformatics 19:299–300.

Dunn, C. W. 2005. The complex colony-level organization of the deep-sea siphonophore Bargmannia elongata (Cnidaria, Hydrozoa) is directionally asymmetric and arises by the subdivision of pro-buds. Dev. Dyn. 234:835–845.

Dunn, C. W., P. R. Pugh, and S. H. D. Haddock. 2005. *Marrus claudanielis*, a new species of deep-sea physonect siphonophore (Siphonophora, Physonectae). Bull. Mar. Sci. 76:699–714.

Farris, J., M. Källersjö, A. Kluge, and C. Bult. 1995. Testing significance of incongruence. Cladistics 10:315–319.

Fewkes, J. W. 1880. Contributions to a knowledge of tubular jellyfishes. Bull. Mus. Comp. Zoo. Harvard 6:127–146.

Force, A., M. Lynch, F. B. Pickett, A. Amores, Y. L. Yan, and J. Postlethwait. 1999. Preservation of duplicate genes by complementary, degenerative mutations. Genetics 151:1531–1545.

Garstang, W. 1946. The morphology and relations of the Siphonophora. Quart. J. Micr. Sci. 87:103–193.

Gasca, R. 2002. Lista faunistica y bibliografia comentadas de los sifonoforos (Cnidaria: Hydrozoa) de Mexico. An. Inst. Biol. Univ. Nac. Auton. Mex. (Zool.) 73:123–143.

Gegenbaur, K. 1859. Neue Beiträge zur näheren Kenntniss der Siphonophoren. Z. Wissen. Zool. 5:285–344.

Goldman, N., J. P. Anderson, and A. G. Rodrigo. 2000. Likelihood-based tests of topologies in phylogenetics. Syst. Biol. 49:652–670.

Haddock, S. H. D., C. W. Dunn, and P. R. Pugh. 2005. A reexamination of siphonophore terminology and morphology, applied to the description of two new prayine species with remarkable bio-optical properties. J. Mar. Biol. Assoc. U.K. 85:695–707.

Haeckel, E. 1869. Ueber Arbeitstheilung in Natur-und Menschenleben. Berliner Handwerker-Vereins, Berlin.

Haeckel, E. 1888. Report on the Siphonophorae collected by H.M.S. Challenger during the years 1873–1876. Report of the Scientific

Research Exploring Voyage of H.M.S. "Challenger," 1873–1876. Zoology 28:1–380.
Hamner, W. M. 1975. Underwater observations of blue-water plankton: Logistics, techniques, and safety procedures for divers at sea. Limnol. Oceanogr. 20:1045–1051.
Harvell, C. D. 1994. The evolution of polymorphism in colonial invertebrates and social insects. Q. Rev. Biol. 69:155–185.
Hassanin, A., G. Lecointre, and S. Tillier. 1998. The 'evolutionary signal' of homoplasy in protein-coding gene sequences and its consequences for a priori weighting in phylogeny. C. R. Acad. Sci. Paris Life Sci. 321:611–620.
Hillis, D. M., B. K. Mable, and C. Moritz. 1996. Applications of molecular systematics: The state of the field and a look to the future. Pages 515–543 *in* Molecular systematics, second edition (D. M. Hillis, C. Moritz, and B. K. Mable, eds.). Sinauer Associates, Sunderland, Massachusetts.
Hissmann, K. 2005. *In situ* observations on benthic siphonophores (Physonectae: Rhodaliidae) and descriptions of three new species from Indonesia and South Africa. Syst. Biodivers. 2:223–249.
Huelsenbeck, J. P., D. M. Hillis, and R. Jones. 1996. Parametric bootstrapping in molecular phylogenetics: Applications and performance. Pages 19–45 *in* Molecular zoology: Advances, strategies, and protocols (J. D. Ferraris, and S. R. Palumbi, eds.). Wiley-Liss, Chichester, UK.
Huxley, T. H. 1859. The oceanic Hydrozoa; a description of the Calycophoridae and Physophoridae observed during the voyage of H.M.S. "Rattlesnake," in the years 1846–1850. Ray Society, London.
Kawamura, T. 1910. "Bozunira" and "Katsuwo no Eboshi," *Rhizophysa* and *Physalia*. Dobutz Z. Tokyo 22:445–454.
Leloup, E. 1954. A propos des Siphonophores. Volume Jubilaire, Victor van Straelan, Bruxelles. 2:643–699.
Lewis, P. O. 2001. A likelihood approach to estimating phylogeny from discrete morphological character data. Syst. Biol. 50:913–925.
Mackie, G. O. 1963. Siphonophores, bud colonies, and superorganisms. Pages 329–337 *in* The Lower Metazoa (E. Dougherty, ed.). University of California Press, Berkeley.
Mackie, G. O., P. R. Pugh, and J. E. Purcell. 1987. Siphonophore biology. Adv. Mar. Biol. 24:97–262.
Maddison, D., and W. Maddison. 2003. MacClade, version 4.06. Sinauer, Sunderland, Massachusetts.
Maddison, W., and D. Maddison. 2004. Mesquite: A modular system for evolutionary analysis. Version 1.04. www.mesquiteproject.org.
Mapstone, G. M. 2004. First full description of the siphonophore *Halistemma amphytridis* (Lesueur and Petit, 1807). Hydrobiologia 530/531:231–240.
McShea, D., and E. Venit. 2002. Testing for bias in the evolution of coloniality: A demonstration in cyclostome bryozoans. Paleobiology 28:308–327.
Medina, M., A. G. Collins, J. D. Silberman, and M. L. Sogin. 2001. Evaluating hypotheses of basal animal phylogeny using complete sequences of large and small subunit rRNA. Proc. Natl. Acad. Sci. USA 98:9707–9712.
Medlin, L., H. J. Elwood, S. Stickel, and M. L. Sogin. 1988. The characterization of enzymatically amplified eukaryotic 16S-like rRNA-coding regions. Gene 71:491–499.
Metschnikoff, E. 1874. Studien über die Entwickelung der Medusen und Siphonophoren. Z. Wissen. Zool. 24:15–83.
Notredame, C., D. G. Higgins, and J. Heringa. 2000. T-Coffee: A novel method for fast and accurate multiple sequence alignment. J. Mol. Biol. 302:205–217.
Nylander, J. A. A. 2002. MrModeltest v1.1b. Program distributed by the author. Department of Systematic Zoology, Uppsala University.
Page, R. D. 1996. TREEVIEW: An application to display phylogenetic trees on personal computers. Comput. Appl. Biosci. 12:357–358.
Page, R. D. 2000. Circles: Automating the comparative analysis of RNA secondary structure. Bioinformatics 16:1042–1043.
Pagel, M. 1994. Detecting correlated evolution on phylogenies: A general method for the comparative analysis of discrete characters. Proc. Roy. Soc. B 255:37–45.
Pagel, M. 1997. Inferring evolutionary processes from phylogenies. Zool. Scripta 26:331–348.
Pagel, M., A. Meade, and D. Barker. 2004. Bayesian estimation of ancestral character states on phylogenies. Syst. Biol. 53:673–684.
Pagès, F., and J.-M. Gili. 1992. Siphonophores (Cnidaria, Hydrozoa) of the Benguela Current (southeastern Atlantic). Sci. Mar. 56 (Suppl. 1):65–112.
Philippe, H., and P. Forterre. 1999. The rooting of the universal tree of life is not reliable. J. Mol. Evol. 49:509–523.
Philippe, H., U. Sörhannus, A. Baroin, R. Perasso, F. Gasse, and A. Adoutte. 1994. Comparison of molecular and paleontological data in diatoms suggests a major gap in the fossil record. J. Evol. Biol. 7:247–265.
Pont-Kingdon, G., C. G. Vassort, R. Warrior, R. Okimoto, C. T. Beagley, and D. R. Wolstenholme. 2000. Mitochondrial DNA of *Hydra attenuata* (Cnidaria): A sequence that includes an end of one linear molecule and the genes for l-rRNA, tRNA(f-Met), tRNA(Trp), COII, and ATPase8. J. Mol. Evol. 51:404–415.
Posada, D., and K. Crandall. 1998. ModelTest: Testing the model of DNA substitution. Bioinformatics 14:817–818.
Pugh, P. R. 1983. Benthic siphonophores: A review of the family Rhodaliidae (Siphonophora, Physonectae). Phil. Trans. R. Soc. Lond. B Biol. Sci. 301:165–300.
Pugh, P. R. 1992. A revision of the sub-family Nectopyramidinae (Siphonophora, Prayidae). Phil. Trans. R. Soc. Lond. B Biol. Sci. 335:281–322.
Pugh, P. R. 1998. A re-description of *Frillagalma vityazi* Daniel 1966 (Siphonophorae, Agalmatidae). Sci. Mar. 62:233–245.
Pugh, P. R. 1999. A review of the genus *Bargmannia* Totton, 1954 (Siphonophorae, Physonecta, Pyrostephidae). Bull. Nat. Hist. Mus. Zool. Ser. 65:51–72.
Pugh, P. R. 2001. A review of the genus *Erenna* Bedot, 1904 (Siphonophora, Physonectae). Bull. Nat. Hist. Mus. Zool. Ser. 67:169–182.
Pugh, P. R. 2003. A revision of the family Forskaliidae (Siphonophora, Physonectae). J. Nat. Hist. 37:1281–1327.
Pugh, P. R. 2005. A new species of *Physophora* (Siphonophora: Physonectae: Physophoridae) from the North Atlantic, with comments on related species. Syst. Biodivers. 2:251–270.
Rambaut, A., and A. Drummond. 2003. Tracer v1.0, available from www.evolve.zoo.ox.ac.uk.
Rambaut, A., and N. C. Grassly. 1997. Seq-Gen: an application for the Monte Carlo simulation of DNA sequence evolution along phylogenetic trees. Comput. Appl. Biosci. 13:235–238.
Robison, B. H. 1995. Light in the Ocean's Midwaters. Sci. Am. 273:60–64.
Ronquist, F., and J. P. Huelsenbeck. 2003. MrBayes 3: Bayesian phylogenetic inference under mixed models. Bioinformatics 19:1572–1574.
Schneider, K. C. 1896. Mittheilungen über Siphonophoren. II. Grundriss der organization der Siphonophoren. Zool. J. Abt. Anat. 9:571–664.
Schuchert, P. 2005. Species boundaries in the hydrozoan genus *Coryne*. Mol. Phylogenet. Evol. 36:194–199.
Stajich, J. E., D. Block, K. Boulez, S. E. Brenner, S. A. Chervitz, C. Dagdigian, G. Fuellen, J. G. Gilbert, I. Korf, H. Lapp, H. Lehvaslaiho, C. Matsalla, C. J. Mungall, B. I. Osborne, M. R. Pocock, P. Schattner, M. Senger, L. D. Stein, E. Stupka, M. D. Wilkinson, and E. Birney. 2002. The Bioperl toolkit: Perl modules for the life sciences. Genome Res. 12:1611–1618.
Stepanjants, S. 1967. Siphonophores of the seas of the USSR and the north western part of the Pacific Ocean. Opredeliteli po Faune SSSR 96:1–216.
Swofford, D. 2003. PAUP*: Phylogenetic analysis using parsimony (*and Other Methods), Version 4. Sinauer Associates, Sunderland, Massachusetts.
Totton, A. K. 1936. Plankton of the Bermuda Oceanographic Expeditions. VII. Siphonophora taken during the year 1931. Zoologica 21:231–240.
Totton, A. K. 1954. Siphonophora of the Indian Ocean. Discov. Rep. 27:1–162.
Totton, A. K. 1960. Studies on *Physalia physalis* Part 1. Natural History and Morphology. Discov. Rep. 30:301–368.
Totton, A. K. 1965. A synopsis of the Siphonophora. British Museum of Natural History, London.

Wilson, E. O. 2000. Sociobiology: The new synthesis. Belknap Press, Cambridge, UK.

Youngbluth, M. 1984. Manned submersibles and sophisticated instrumentation: Tools for oceanographical research. Pages 335–344 *in* Proceedings of SUBTECH '83 Symposium Society for Underwater Technology, London.

Zuker, M. 2003. Mfold web server for nucleic acid folding and hybridization prediction. Nucleic Acids Res. 31:3406–3415.

First submitted 11 November 2004; reviews returned 8 March 2005; final acceptance 27 June 2005

Associate Editor: Gavin Naylor

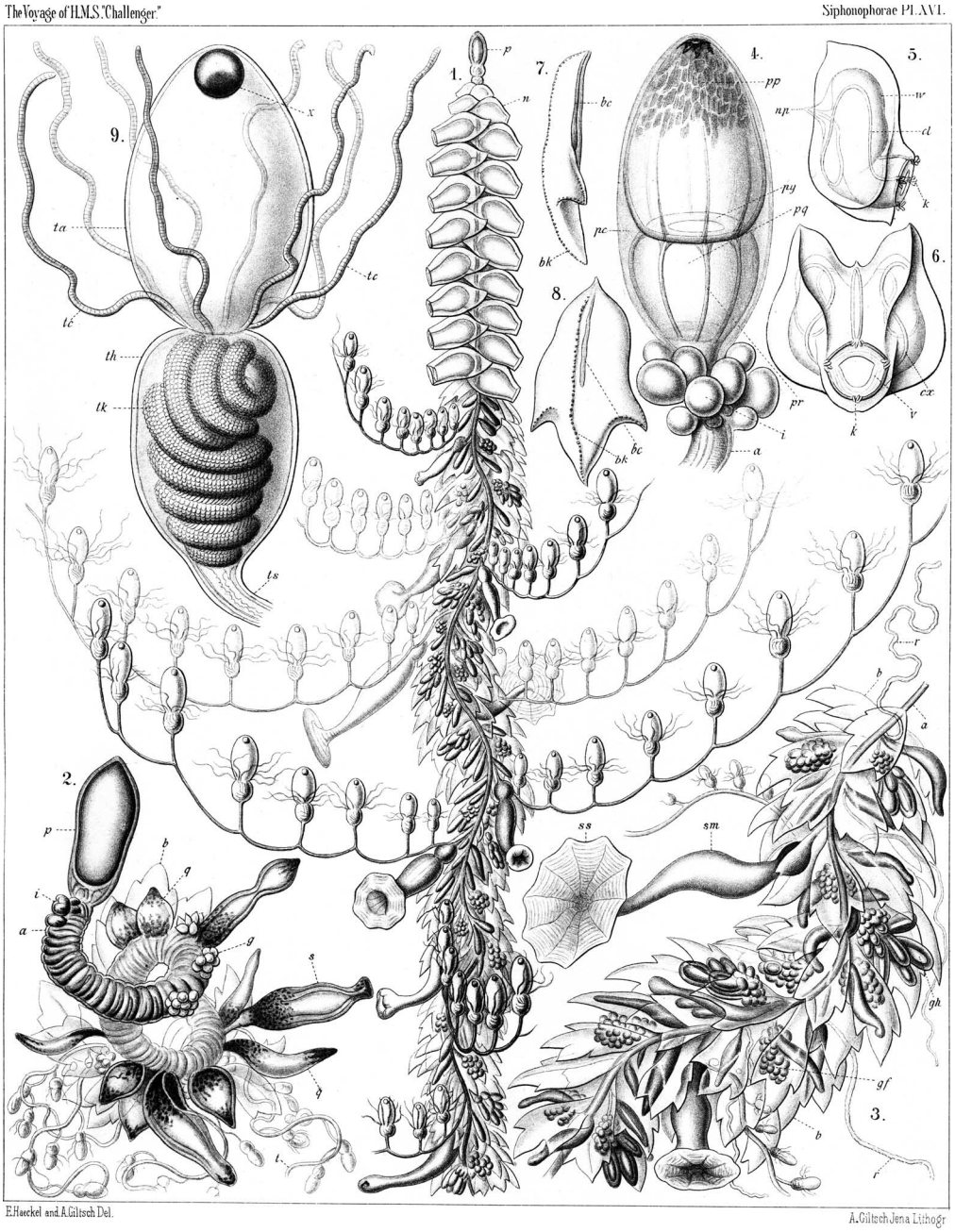

Haeckel's illustration of the physonect *Lychnagalma vesicularia*, a species he described in his monograph on siphonophores (Haeckel, 1888). This species has since been synonymized with *L. utricularia*. (1) The entire colony. (2) The twisted stem of a specimen that has lost most of its zooids. (3) Detail of a portion of the siphosome. (4) The pneumatophore, with nectophore buds to its posterior. (5–8) Nectophores and bracts. (9) Detail of a tentillum(the side-branch of a gastrozooid tentacle), which has a buoyant terminal vesicle unique to this species. *L. utricularia* was collected only several times prior to the development of modern research submersibles.